Eric keller

DRAFT REPORT

TL-1 Curb-Type Bridge Railing for Longitudinal Glulam Timber Decks Located on Low-Volume Roads

Submitted by

Ronald K. Faller, P.E.
Research Associate Engineer

Ketil Soyland
Graduate Research Assistant

Barry T. Rosson, Ph.D., P.E.
Assistant Professor

Tyler M. Stutzman
Mechanical Engineering Student

MIDWEST ROADSIDE SAFETY FACILITY
Center for Infrastructure Research
Civil Engineering Department
University of Nebraska-Lincoln
1901 "Y" Street, Building "C"
Lincoln, Nebraska 68588-0601
(402) 472-6864

submitted to

Michael A. Ritter, P.E.
Structural Engineer

U.S. Department of Agriculture
Forest Service
Forest Products Laboratory
One Gifford Pinchot Dr.
Madison, Wisconsin 53705
(608) 231-9229

MwRSF Research Report No. TRP-03-54-96

April 1996

DISCLAIMER STATEMENT

The contents of this report reflect the views of the authors who are responsible for the facts and the accuracy of the data presented herein. The contents do not necessarily reflect the official views or policies of the United States Department of Agriculture, Forest Service, Forest Products Laboratory. This report does not constitute a standard, specification, or regulation.

ACKNOWLEDGMENTS

The authors would like to thank the following organizations who have contributed to the success of this research project: the American Institute of Timber Construction (AITC), Vancouver, WA, for donating the glulam materials used for the deck construction; and the Office of Sponsored Programs and the Center for Infrastructure Research, University of Nebraska-Lincoln, Lincoln, NE for matching support.

A special thanks is also given to the following individuals who made a contribution to the completion of this research project.

Midwest Roadside Safety Facility

Dean L. Sicking, Ph.D., P.E., MwRSF Director and Assistant Professor
Brian G. Pfeifer, P.E., Research Associate Engineer
James C. Holloway, Research Associate Engineer
Kenneth L. Krenk, Field Operations Manager
Eric Keller, Computer Technician II
Undergraduate and Graduate Assistants

Dunlap Photography

James Dunlap, President and Owner

ABSTRACT

A low-height, curb-type timber bridge railing was developed for use on longitudinal timber bridge decks located on low-volume roads. A 6¾-in. x 10½-in. (171-mm x 267-mm) curb rail was supported by timber scupper blocks spaced on 10-ft (3048-mm) centers. The height to the top of the railing was 17¾ in. (451 mm). The research study included 6 static tests and one full-scale vehicle crash test. The curb-type bridge railing successfully redirected a 3/4-ton pickup truck impacting at a speed of 31.1 mph (50 km/hr) and at an angle of 25 degrees. The safety performance of the bridge railing was acceptable according to the Test Level 1 (TL-1) evaluation criteria described in the National Cooperative Highway Research Report No. 350, *Recommended Procedures for the Safety Performance Evaluation of Highway Features*.

TABLE OF CONTENTS

List of Figures

List of Tables

1 INTRODUCTION

1.1 Problem Statement

Historically, bridge railing systems have been not been developed for use on low-speed, low-volume roads; however, many U.S. Forest Service and National Forest utility and service roads often carry very low traffic volumes at operating speeds of 20 mph (32.2 km/hr) or less. These roads are often narrow, generally incorporating one- or two-lane timber bridges, with span lengths between 15 and 35 ft (4.6 to 10.7 m). The bridge rails that have been designed for high-speed facilities may be too expensive for low-volume roads. In recognition of the need to develop bridge railings for this low service level, the United States Department of Agriculture (USDA) Forest Service, Forest Product Laboratory (FPL) in cooperation with the Midwest Roadside Safety Facility (MwRSF), undertook the task of developing one low-service level bridge railing system.

1.2 Objective

The objective of this research was to develop a low-cost, low-height, curb-type timber bridge railing system for use on longitudinal timber decks with low traffic volumes and speeds. The bridge railing was developed to meet the Test Level 1 (TL-1) evaluation criteria described in the National Cooperative Highway Research Report No. 350, *Recommended Procedures for the Safety Performance Evaluation of Highway Features* (1). A longitudinal glulam timber deck was selected for use in the development of the bridge railing because it is the weakest type of longitudinal timber deck currently in use for resisting transverse railing loads. Thus, any bridge railing not damaging the longitudinal glulam deck could easily be adapted to other, stronger, timber deck systems.

1.3 Scope

The research objective was achieved by performing several tasks. First, a literature review was performed on existing curb-type timber bridge railings and barriers, as well as bridge railings developed for timber deck bridges. Second, static testing was performed on the several types of rail-to-post connections. Third, an analysis and design phase was performed on all structural members and connections. Fourth, computer simulation modeling was conducted on the final bridge railing design. One full-scale vehicle crash test was then performed using a 3/4-ton pickup truck, weighing approximately 4,409 lbs (2000 kg), with a target impact speed and angle of 31.1 mph (50 km/h) and 25 degrees, respectively. Finally, the test results were analyzed, evaluated and documented, with conclusions and recommendations pertaining to the safety performance of the curb-type bridge railing.

2 LITERATURE REVIEW

2.1 Bridge Railings for Timber Deck Bridges

Over the past seven years, MwRSF and FPL have designed and developed several bridge railings and transitions for use on longitudinal glulam timber bridge decks. Seven bridge railings have been developed for several design impact conditions, including AASHTO Performance Levels 1 and 2 (2), NCHRP 350 Test Levels 1 and 4 (1), as well as for very low-speed, low-volume roadways (3-8). The bridge railing systems developed for timber decks include: (1) an AASHTO PL-1 Glulam Rail with Curb bridge railing (3-6); (2) an AASHTO PL-1 Glulam Rail without Curb bridge railing (3-6); (3) an AASHTO PL-1 Steel Thrie-Beam Rail bridge railing (3-6); (4) an AASHTO PL-2 Steel Thrie-Beam with top-mounted Channel Rail bridge railing (4-7); (5) a NCHRP 350 TL-4 Glulam Rail with Curb bridge railing (4-7); (6) a NCHRP 350 TL-1 low-cost Breakaway W-Beam bridge railing (8); and (7) a Low-Height Curb-Type bridge railing for low-speed, low-volume roads (8).

Two other research programs conducted in the United States provided information on the crashworthiness of bridge railings for use on timber deck bridges. The first program was performed at Southwest Research Institute (SwRI) in the late 1980's in which crash tests were conducted according to AASHTO Performance Level 1 on a glulam rail with a curb bridge railing system attached to a spike-laminated longitudinal timber bridge deck (9). In 1993, a second research project was conducted by the Constructed Facilities Center (CFC) at West Virginia University with crash testing performed by the Texas Transportation Institute (TTI). Crash tests were performed according to AASHTO Performance Level 1 on three bridge railing systems and one transition system attached to a transverse glulam timber deck (10-13).

2.2 Temporary Curb-Type Timber Barriers and Bridge Railings

In the late 1970's, several research studies were directed toward the development of temporary curb-type timber barriers. In the first study, SwRI conducted two crash tests on a 10-in. x 10-in. (254-mm x 254-mm) timber barrier using large sedans impacting at speeds between 35 and 39 mph (56 and 62 km/hr) and angles between 7 and 15 degrees (14). From the crash test results, the SwRI researchers concluded that temporary timber curb barriers provided minimal redirection capability, but could be used for very low speed operations, where speeds and impact angles are low and traffic consists of automobiles.

During the next study, the New York State Department of Transportation (NYSDOT) performed eight crash tests with mid-size sedans on two timber curb configurations - a 12-in. x 12-in. (305-mm x 305-mm) curb and a 16-in. x 10-in. (406-mm x 254-mm) curb with W-Beam attached to the front vertical face (15). For the 12-in. x 12-in. (305-mm x 305-mm) curb, six crash tests were performed at impact speeds between 10 and 30 mph (16 and 48 km/hr) and angles between 3 and 7.5 degrees. The results of these tests indicated that the 12-in. x 12-in. (305-mm x 305-mm) curb was unable to redirect vehicles even in moderate impacts, although the anchorage system did prevent barrier movement. For the 16-in. x 10-in. (406-mm x 254-mm) curb with attached W-Beam, two crash tests were performed at impact speeds between 38 and 47 mph (61 and 76 km/hr) and angles between 14 and 17 degrees. The results of these tests indicated that the 16-in. x 10-in. (406-mm x 254-mm) curb provided satisfactory redirection for impact speeds up to 40 mph (64 km/hr) and angles of 15 degrees. Also mentioned in this paper, NYSDOT developed and tested a temporary timber curb bridge railing, consisting of two 12-in. x 12-in. (305-mm x 305-mm) curb rails stacked vertically and bolted through a bridge deck. The

railing system successfully redirected a large sedan impacting at 52 mph (84 km/hr) and 13 degrees.

3 TEST REQUIREMENTS AND EVALUATION CRITERIA

3.1 Test Requirements

Until recently, bridge railings were typically designed to satisfy the requirements provided in the American Association of State Highway and Transportation Official's (AASHTO's) *Guide Specifications for Bridge Railings* (2). More specifically, bridge railings were designed according to the appropriate performance level of the roadway, based upon a number of factors such as design speed, average daily traffic (ADT), percentage of trucks, bridge rail offset, and number of lanes. These guide specifications included three performance levels, as shown in Table 1, which provided criteria for evaluating the safety performance of bridge railings.

The recently published NCHRP Report No. 350 (1) provides for six test levels, as shown in Table 1, for evaluating longitudinal barriers. Although this document does not contain objective criteria for where each test level is to be used, safety hardware developed to meet the lower test levels are generally intended for use on lower service level roadways while higher test level hardware is intended for use on higher service level roadways. The lowest performance level, Test Level 1 (TL-1), is suitable for applications on low-volume, low-speed facilities such as residential streets. Thus, test impact conditions from Test Level 1 were chosen for the curb-type bridge railing system envisioned. Test Level 1 requires that the bridge railing meet two full-scale vehicle crash tests: (1) an 1,808-lb (820-kg) small car impacting at 31.1 mph (50 km/hr) and 20 degrees; and (2) a 4,409-lb (2,000-kg) pickup truck impacting at a speed of 31.1 mph (50 km/hr) and 25 degrees.

Table 1. AASHTO Crash Test Conditions for Bridge Railings (2) and NCHRP 350 Crash Test Conditions for Longitudinal Barriers (1)

AASHTO Performance Level (2)	Impact Conditions				
	Small Car (816 kg)	Pickup Truck (2,449 kg)	Medium Single-Unit Truck (8,165 kg)	Van-Type Tractor-Trailer (22,680 kg)	
1	80.5 km/h and 20 deg	72.4 km/h and 20 deg			
2	96.6 km/h and 20 deg	96.6 km/h and 20 deg	80.5 km/h and 15 deg		
3	96.6 km/h and 20 deg	96.6 km/h and 20 deg		80.5 km/h and 15 deg	
NCHRP 350 Test Level (1)	Impact Conditions				
	Small Car (820 kg)	Pickup Truck (2,000 kg)	Single-Unit Van Truck (8,000 kg)	Tractor/Van Trailer (36,000 kg)	Tractor/Tank Trailer (36,000 kg)
1	50 km/h & 20 deg	50 km/h & 25 deg			
2	70 km/h & 20 deg	70 km/h & 25 deg			
3 (Basic Level)	100 km/h & 20 deg	100 km/h & 25 deg			
4	100 km/h & 20 deg	100 km/h & 25 deg	80 km/h & 15 deg		
5	100 km/h & 20 deg	100 km/h & 25 deg		80 km/h & 15 deg	
6	100 km/h & 20 deg	100 km/h & 25 deg			80 km/h & 15 deg

3.2 Evaluation Criteria

Evaluation criteria for full-scale vehicle crash testing are based on three appraisal areas: (1) structural adequacy; (2) occupant risk; and (3) vehicle trajectory after collision. Criteria for structural adequacy are intended to evaluate the ability of the railing to contain, redirect, or allow controlled vehicle penetration in a predictable manner. Occupant risk evaluates the degree of hazard to occupants in the impacting vehicle. Vehicle trajectory after collision is a measure of the potential for the post-impact trajectory of the vehicle to cause subsequent multi-vehicle accidents, thereby subjecting occupants of other vehicles to undue hazard or to subject the occupants of the impacting vehicle to secondary collisions with other fixed objects. These three evaluation criteria are defined in Table 2.

Table 2. NCHRP Report 350 Evaluation Criteria for 2000P Pickup Truck Crash Test (1).

Structural Adequacy	A.	Test article should contain and redirect the vehicle; the vehicle should not penetrate, underride, or override the installation although controlled lateral deflection of the test article is acceptable.
Occupant Risk	D.	Detached elements, fragments or other debris from the test article should not penetrate or show potential for penetrating the occupant compartment, or present an undue hazard to other traffic, pedestrians, or personnel in a work zone. Deformations of, or intrusions into, the occupant compartment that could cause serious injuries should not be permitted.
	F.	The vehicle should remain upright during and after collision although moderate roll, pitching, and yawing are acceptable.
Vehicle Trajectory	K.	After collision it is preferable that the vehicle's trajectory not intrude into adjacent traffic lanes.
	L.	The occupant impact velocity in the longitudinal direction should not exceed 12 m/sec and the occupant ridedown acceleration in the longitudinal direction should not exceed 20 G's.
	M.	The exit angle from the test article preferably should be less than 60 percent of test impact angle, measured at time of vehicle loss of contact with test devise.

4 DEVELOPMENT AND DESIGN

4.1 Dynamic Lateral Impact Force

The design of the low-volume curb-type bridge railing required an estimate of the dynamic lateral impact force applied to the railing. Two common methods were used: (1) an approximate method to predict the lateral impact force using a mathematical model taken from NCHRP Report No. 86 (16) and the 1977 AASHTO Barrier Guide (17), and (2) an approximate method using impulse - momentum equations and the coefficient of restitution.

The first method or mathematical model (16,17) is presented in Equations 1 and 2 by:

$$F_{lat.\ ave.} = \frac{W\ V_I^2\ \sin^2\theta}{2g\,[A\,L\sin\theta - B\,(1-\cos\theta) + D]} \quad \textbf{(1)}$$

and

$$F_{lat.\ peak} = F_{lat.\ ave}\ x\ DF \quad \textbf{(2)}$$

where
$F_{lat.\ ave.}$ = average lateral impact force (lbs)
$F_{lat.\ peak}$ = peak lateral impact force (lbs)
W = vehicle weight (4,409 lbs)
V_I = impact velocity (45.72 ft/sec)
θ = impact angle (25 degrees)
g = acceleration due to gravity (32.2 ft/sec^2)
AL = distance from vehicle's front end to center of mass (8.66 ft)
2B = vehicle width (6.5 ft)
D = lateral displacement of railing (assumed 0 ft)
DF = dynamic factor ($\pi/2$ to 2)

The equations above estimate the average and peak forces that are applied to the vehicle from the point of initial impact until the vehicle becomes parallel to the barrier. An estimate of the duration of this phase of impact, Δt, is expressed by Equation 3 (16).

$$\Delta t = \frac{[A\,L \sin\theta - B\,(1 - \cos\theta) + D]}{\frac{1}{2} V_I \sin\theta} \qquad (3)$$

For a 4,409-lb (2,000-kg) pickup impacting a bridge railing at a speed of 31.1 mph (50 km/hr) and an angle of 25 degrees, $F_{lat.\ ave}$ can be shown to be 7,618 lbs (33,887 N) and $F_{lat.\ peak}$ ranges from 11,966 lbs to 15,235 lbs (53,227 to 67,768 N). Equation 3 predicts that the vehicle will become parallel to the barrier approximately 0.347 sec after initial impact. The vehicle would be expected to move approximately 14.4 ft (4.39 m) down the rail during this time.

Impulse - momentum equations and the coefficient of restitution can also be used to estimate the lateral impact force. The coefficient of restitution, e, is the ratio between the pre-impact and post-impact velocities as shown in Equation 4. The coefficient of restitution is a measure of the energy absorbed by vehicle and barrier deformations. Higher values indicate less energy absorption and higher impulses imparted to the vehicle. Since the coefficient of restitution cannot be greater than 1, this value gives an upper bound on the impulse imparted on the vehicle and hence yields a measure of the maximum force that can be applied to the barrier.

$$e = \frac{V_{B2} - V_{A2}}{V_{A1} - V_{B1}} = \frac{|\text{relative velocity of separation}|}{|\text{relative velocity of approach}|} \qquad (4)$$

where
V_{A1} = velocity of auto before impact (ft/sec)
V_{A2} = velocity of auto after impact (ft/sec)
V_{B1} = velocity of barrier before impact (ft/sec)
V_{B2} = velocity of barrier after impact (ft/sec)

The impulse, or change in momentum during the impact, is estimated using equations 5 through 7.

$$I = \int_{t_1}^{t_2} F\,dt = M_F - M_I \tag{5}$$

$$M_I = m_A V_{A1} + m_B V_{B1} \tag{6}$$

$$M_F = m_A V_{A2} + m_B V_{B2} \tag{7}$$

where
- I = total impulse
- F = impact force function (lbs)
- t_1 = initial time of impact (sec)
- t_2 = final time of impact (sec)
- M_I = momentum of objects before impact (lb-sec)
- M_F = momentum of objects after impact (lb-sec)
- m_A = mass of vehicle (lb-sec^2/ft)
- m_B = mass of barrier (lb-sec^2/ft)

For an oblique impact between a vehicle and a rigid longitudinal barrier (i.e., mass of barrier infinitely large and velocity of barrier always zero, as shown in Figure 1(a)), Equation 4 can be simplified to:

$$e = \frac{-V_{A2}}{V_{A1}} \tag{8}$$

For an impact at 31.1 mph (50 km/hr) and 25 degrees, V_{A1} is as follows:

$$V_{A1} = 45.72\,\text{fps}(\sin 25^\circ \hat{i} + \cos 25^\circ \hat{j}) = 19.3\,\text{fps}\ \hat{i} + 41.4\,\text{fps}\ \hat{j} \tag{9}$$

(a)

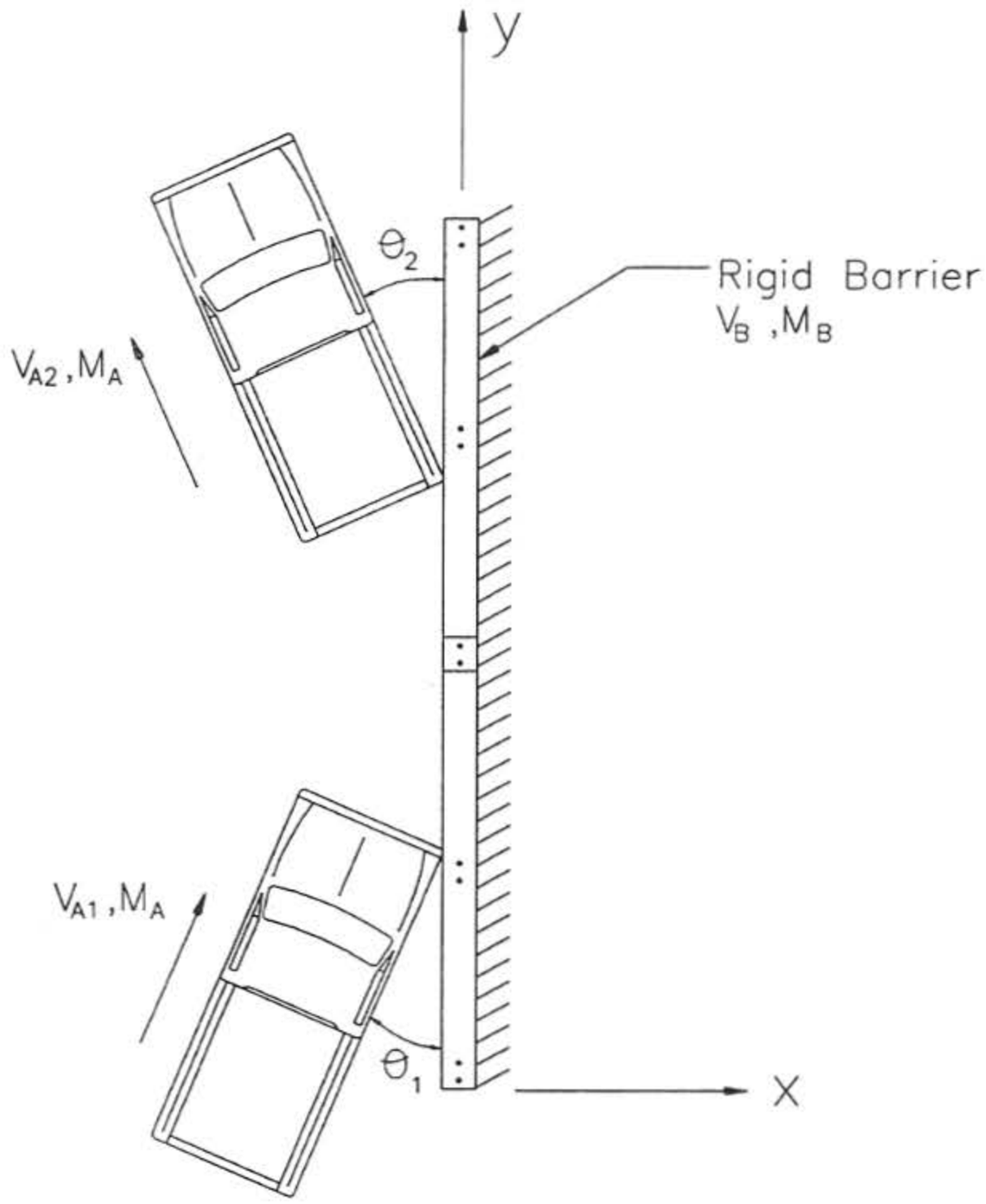

(b)

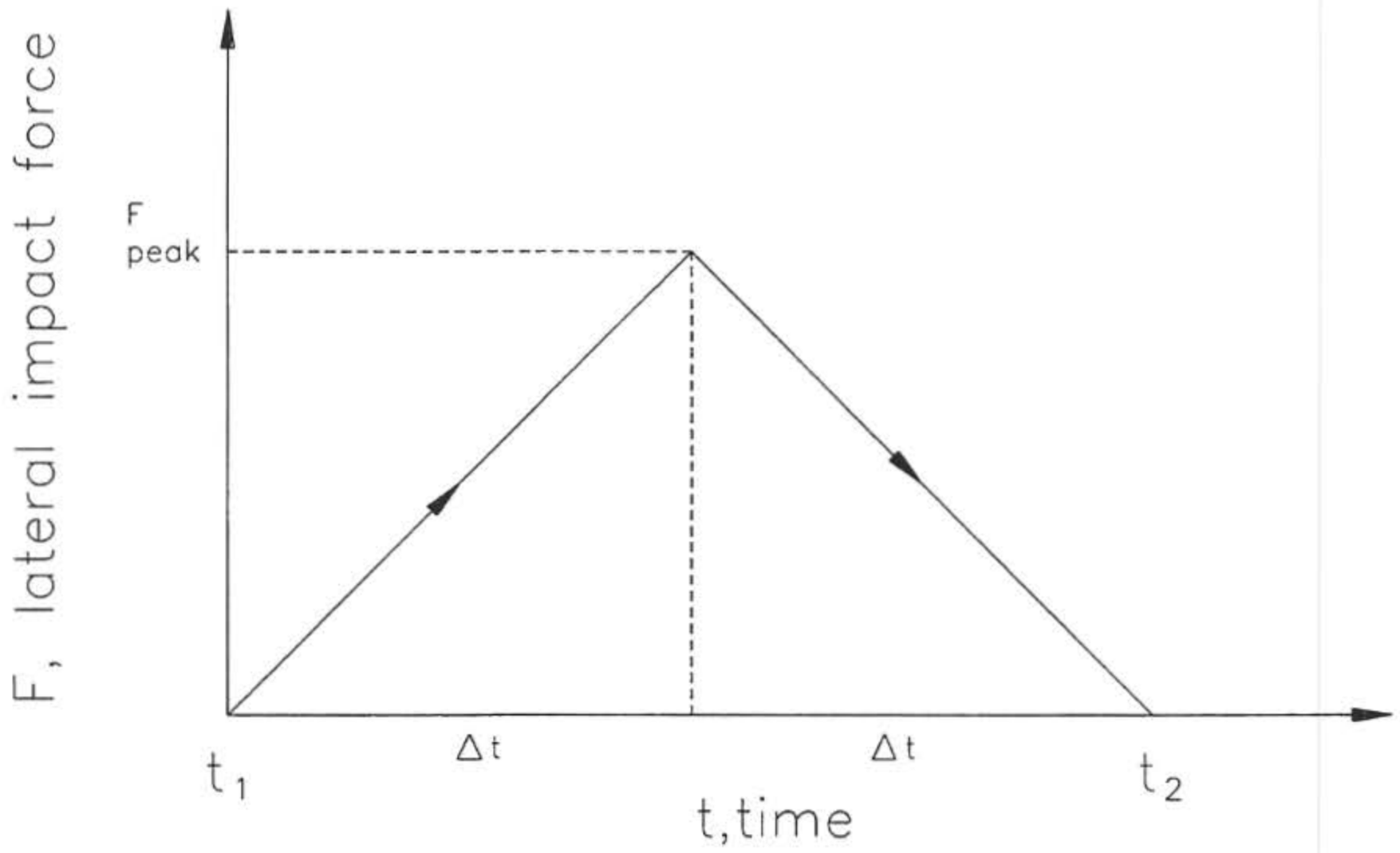

Figure 1. (a) Impact Schematic; and (b) Saw-Tooth Forcing Function

Using the coefficient of restitution, e=1.0, the conservation of momentum in the x-direction, and the x-component of V_{A1} in Equation 9, the x-component of V_{A2} can be found as follows:

$$V_{A2_x} = -19.3\,\text{fps} \tag{10}$$

The momentum in the x-direction before and after impact is shown by Equations 11 and 12.

$$M_{I_x} = m_A V_{A1_x} \tag{11}$$

$$M_{F_x} = m_A V_{A2_x} \tag{12}$$

Using Equations 11 and 12 with a 4,409-lb (2,000-kg) vehicle and substituting into Equation 5, the impulse imparted to the vehicle during impact becomes:

$$\int_{t_1}^{t_2} F_x\,dt = M_{F_x} - M_{I_x} = \left(\frac{4{,}409\,\text{lbs}}{32.2\,\text{ft/sec}^2}\right) \text{x } (-19.3\,\text{fps} - 19.3\,\text{fps}) \tag{13}$$

$$\int_{t_1}^{t_2} F_x\,dt = -5{,}285\,\text{lbs}-\text{sec}$$

Assuming a single, symmetrical saw-tooth forcing function, as shown in Figure 1(b), the impulse is equal to the area under the triangle or $\frac{1}{2}(2\Delta t)F_{\text{lat. peak}}$. If the time from impact until the vehicle becomes parallel to the bridge railing is 0.347 sec, as estimated previously, the peak lateral impact force is estimated to be 15,231 lbs (67,751 N). Thus both procedures predict that the peak lateral impact force should be approximately 15,230 lbs (67,746 N).

4.2 Design Considerations

Timber was selected for use in the curb-type bridge railing based on aesthetics, ease of

construction, and material availability. Since most economical timber curb systems incorporate top-mounted single-railing designs, this type of structure was used for the new bridge rail.

Analysis of vehicular impacts with timber curbs revealed that the curb's shape and top mounting height could effect the redirective capacity of bridge railing system by allowing the vehicle's tire to climb, mount, or traverse the railing. A rectangular curb, with the long dimension oriented perpendicular to the vertical axis, was selected for the rail element since it provided greater economy and increased moment capacity over a square curb. Based on crash tests of previously developed timber curb barriers, the researchers also estimated that 15¾ to 19¾-in. (400 to 502-mm) high curbs should be capable of meeting the desired safety standards (8,14,15). Therefore, it was determined that a top mounting height of 17¾ in. (451 mm), as measured from the top of rail to the top of wearing surface, would be used for the TL-1 curb-type bridge railing, as shown in Figure 2. The 17¾-in. (451-mm) top mounting height of the rail was obtained by using a standard 6¾-in. (171-mm) wide glulam rail element supported by timber scupper blocks measuring 11 in. (279 mm) above the wearing surface.

The peak lateral design force imparted to the curb railing was estimated to be 15,230 lbs (67,746 N) using the procedures described previously. Therefore, it was concluded that the timber curb railing system, when attached to a longitudinal glulam timber deck, should be capable of withstanding the design impact conditions without causing significant damage to the barrier or the timber deck. Delamination and cracking of the glulam deck could be minimized by attaching the rail and scupper blocks to the deck surface with an adequate number of vertical bolts and shear plates (or split rings). Horizontal lag screws, placed into the deck's vertical edge, could also be used to help distribute the lateral impact loads, resulting in tensile stresses in the

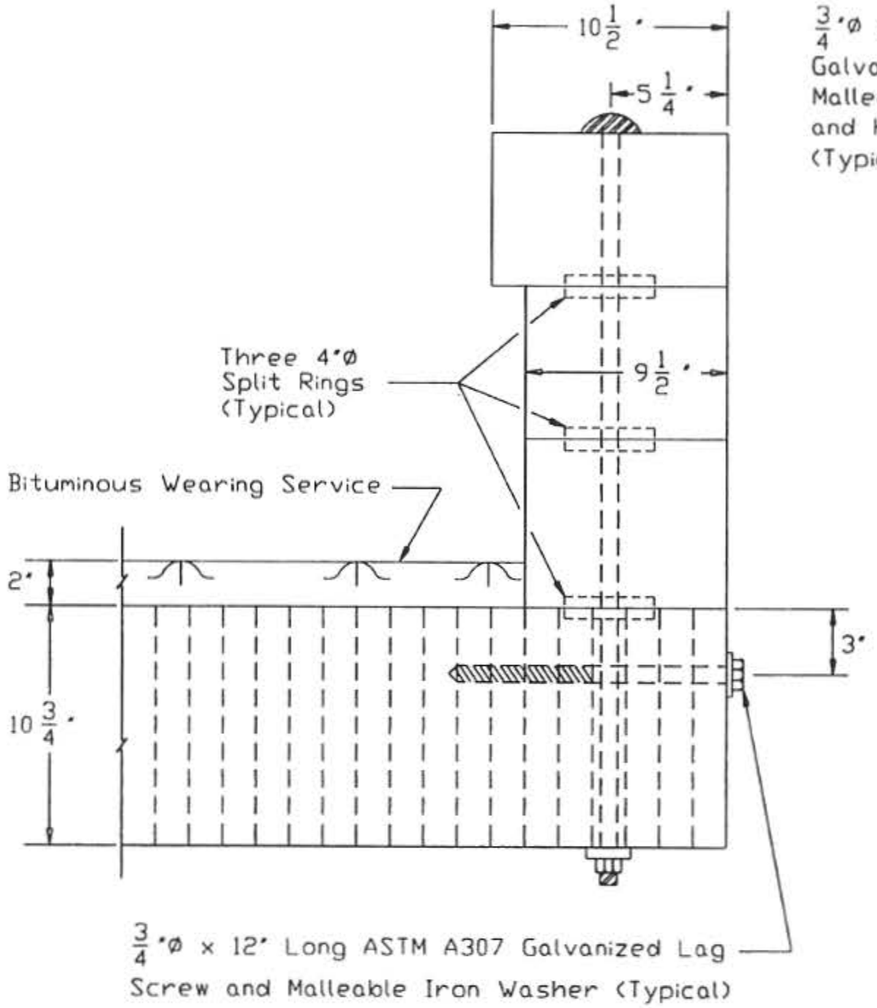

END VIEW

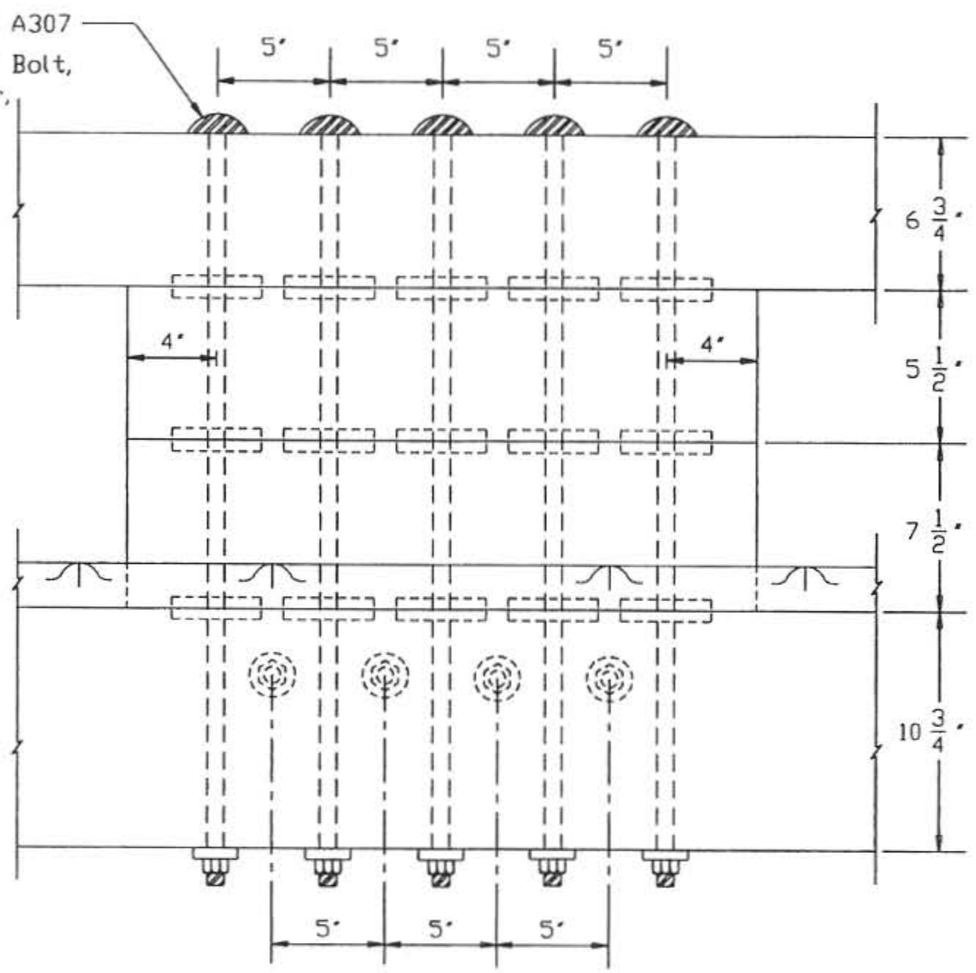

ELEVATION VIEW (Traffic-Side)

Figure 2. Design No. 1 Details

longitudinal deck that are perpendicular to the grain.

4.3 Design No. 1

A preliminary design of the bridge rail (Design No. 1) was made using the lateral design force derived in Section 4.1 and the design considerations discussed in Section 4.2. As shown in Figure 2, a 6¾-in. by 10½-in. (171-mm by 267-mm) timber glulam rail is supported by timber scupper blocks spaced on 10-ft (3048-mm) centers and attached to the surface of the timber bridge deck using five ¾-in. (19-mm) diameter ASTM A307 bolts. All bolted connections between two timber elements are made using either split rings or shear plates. The height from the top of the glulam rail to the top of the asphalt wearing surface is 17¾ in. (451 mm).

5 DEVELOPMENTAL TESTING - PHASE I

5.1 Static Testing

Static testing was used to determine the force-deflection characteristics and the structural capacity of the bolted connection between the glulam rail, scupper blocks, and deck, as shown in Figure 2. The test results could then be used to identity any potential changes in the railing configuration (i.e., reduction in size or quantity of bolts).

The static testing apparatus, as shown in Figure 3, was configured to simulate the bolted connection between the glulam rail, scupper blocks, and bridge deck. A ½-in. (13-mm) thick steel plate was bolted to a concrete foundation and was positioned above the concrete foundation to provide adequate clearance for the heads of the vertical bolts. The scupper blocks and glulam rail were then placed on the vertical bolts using shear plates on each timber surface, except on the top of the glulam rail where malleable iron washers and nuts were used instead.

The static load was applied to the mid-height of the glulam rail's back-side surface using two cables, a steel bar, and a steel bearing plate. A 20-in. (508-mm) stroke, hydraulic ram combined with 1:2 cable pulley system were used to generate the static load, as shown in Figure 3. During testing, a 10,000-lb (44,500-N) capacity, tension load cell and an 80-in. (2032-mm) capacity, string potentiometer were used to measure the load and displacement readings, respectively. The load cell was placed on one side of the pulley and was used to measure one-half of the applied load. A total of three static tests were performed and are described below.

5.1.1 Test No. 1

Test no. 1 was conducted on a configuration consisting of a 6¾-in. (171-mm) high glulam rail supported by two scupper blocks - one 7½-in. (190-mm) high and one 5½-in. (140-

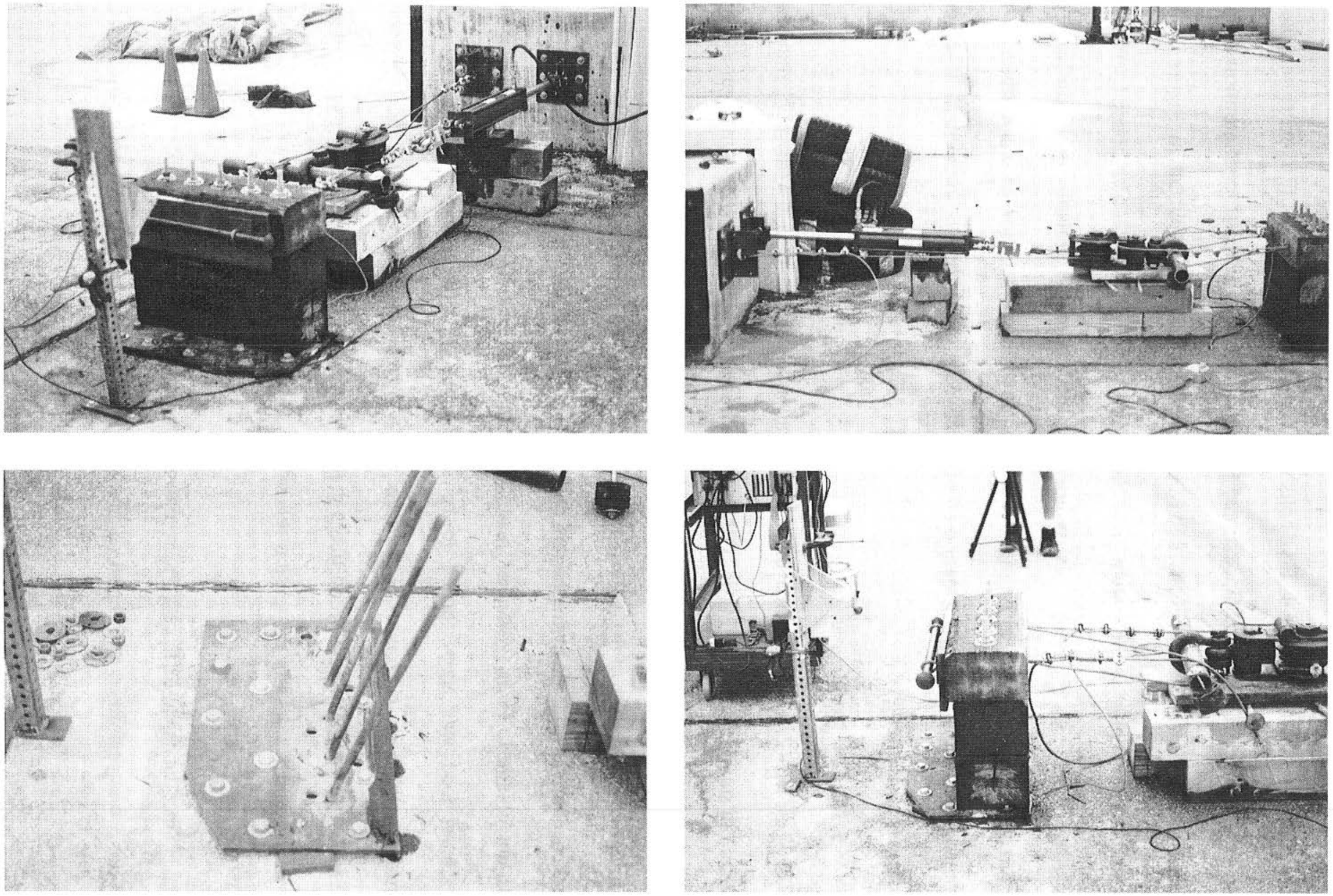

Figure 3. Static Testing Apparatus

mm) high., as shown in Figure 4. Five bolts were placed along the 28-in. (711-mm) long blocks using shear plates at all available locations. Photographs of the deflected configuration are also shown in Figure 4. The force-deflection curve for test no. 1 is provided in Figure 5. The maximum load applied to the system was 15,400 lbs (68,500 N) which corresponded with a rail deflection of 4.9 in. (124 mm), as measured at the top of the glulam rail. Significant rail deformations occurred due to rotations caused by both the compaction of wood fibers in the compression regions and the formation of gaps betweens timber blocks in the tension regions, as shown in Figure 4.

5.1.2 Test No. 2

Test no. 2 was conducted on a configuration consisting of a 6¾-in. (171-mm) high glulam rail supported by two 7½-in. (190-mm) high scupper blocks, as shown in Figure 6. Five bolts were again placed along the 28-in. (711-mm) long blocks using shear plates at all available locations. A photograph of the deflected position is also shown in Figure 6. Technical difficulties were encountered with the hydraulic ram during test no. 2, and therefore a force-deflection curve was not obtained. From voltmeter readings of the load cell and string potentiometer, the maximum load was approximated to be 15,400 lbs (68,500 N) at a rail deflection of approximately 6 in. (152 mm). Significant rail deformations also occurred due to rotations caused by the compaction of wood fibers in the compression regions and the formation of gaps betweens timber blocks in the tension regions, as shown in Figure 6.

5.1.3 Test No. 3

Since technical difficulties were encountered with the hydraulic ram during test no. 2, test no. 3 was performed as a repeat of the railing configuration used in test no. 2, as shown in

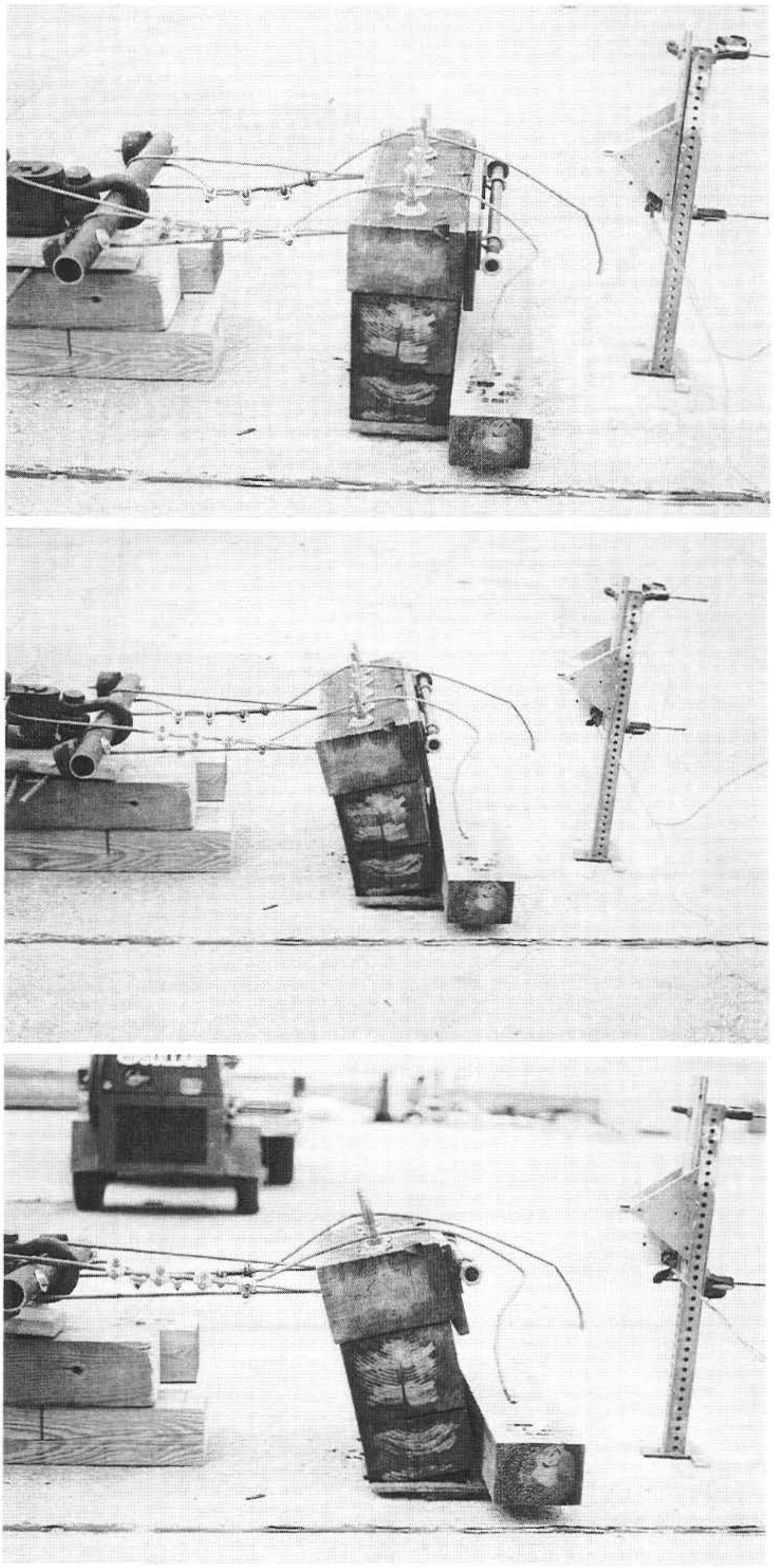

Figure 4. Test No. 1 Configuration and Deflected Position

Figure 5. Force-Deflection Curves for Test Nos. 1 and 3

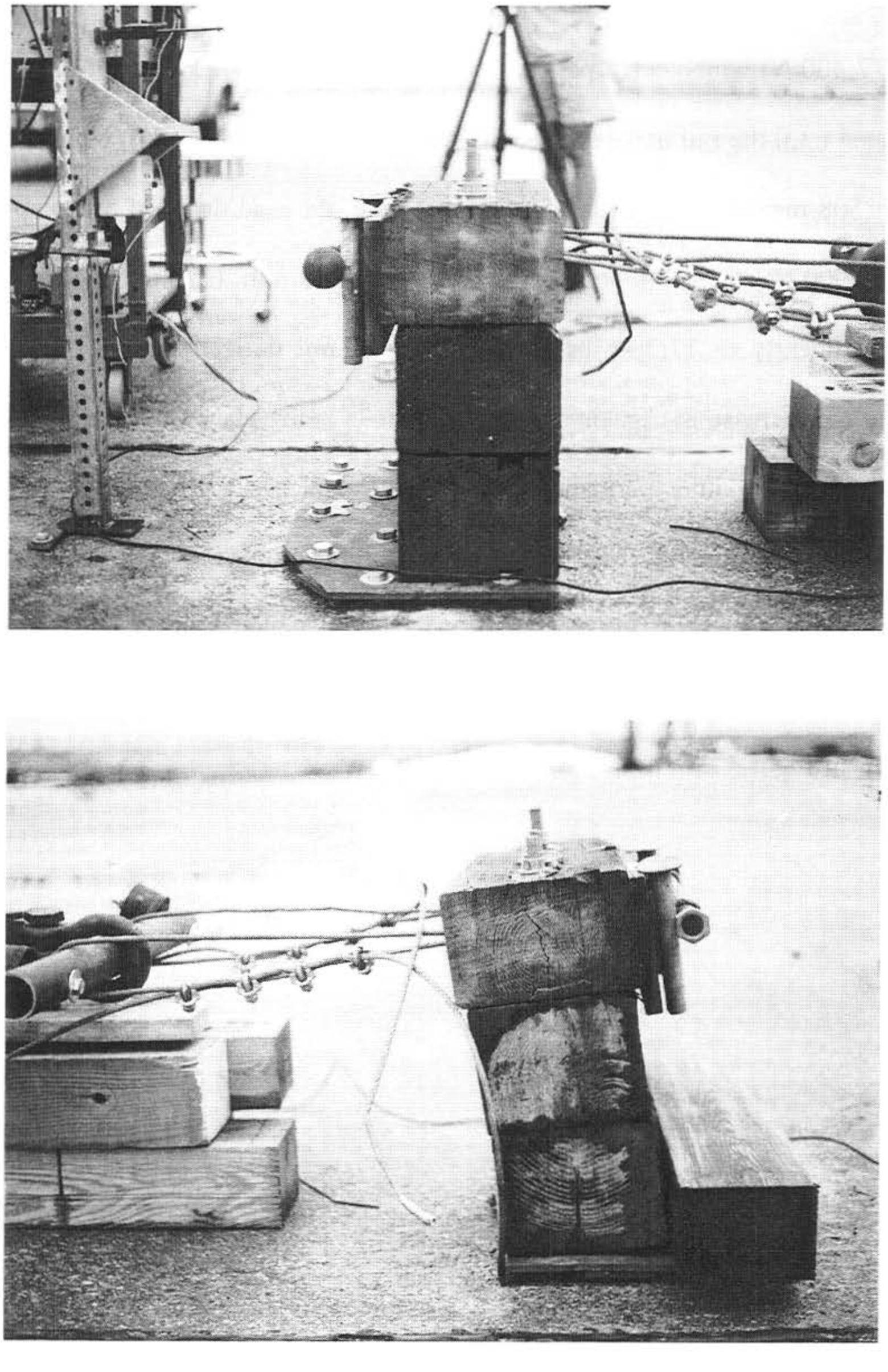

Figure 6. Test No. 2 Configuration and Deflected Position

Figure 7. Photographs of the deflected position are also shown in Figure 7. The force-deflection curve for test no. 3 is provided in Figure 5. The maximum load applied to the system was 17,400 lbs (77,400 N) which corresponded with a rail deflection of 5.7 in. (145 mm). Test no. 3 was continued until the rail had deflected approximately 10 in. (254 mm) or half of the stroke of the 20-in. (508-mm) hydraulic ram. During that time, the load dropped off to approximately 10,100 lbs (44,900 N) at a rail deflection of approximately 6.8 in. (173 mm). Subsequently, the load increased linearly to 17,200 lbs (76,500 N) at a rail deflection of 9.8 in. (249 mm), indicating that the increase in capacity is due to the bolts being placed in tension. The load was then released, resulting in a permanent set of approximately 6.1 in. (155 mm). The rail deformations occurred due to rotations caused by the compaction of wood fibers in the compression regions, the formation of gaps betweens timber blocks in the tension regions, and a combination of tension and shear failures of the lower scupper block propagating from the bolt line, as shown in Figure 7.

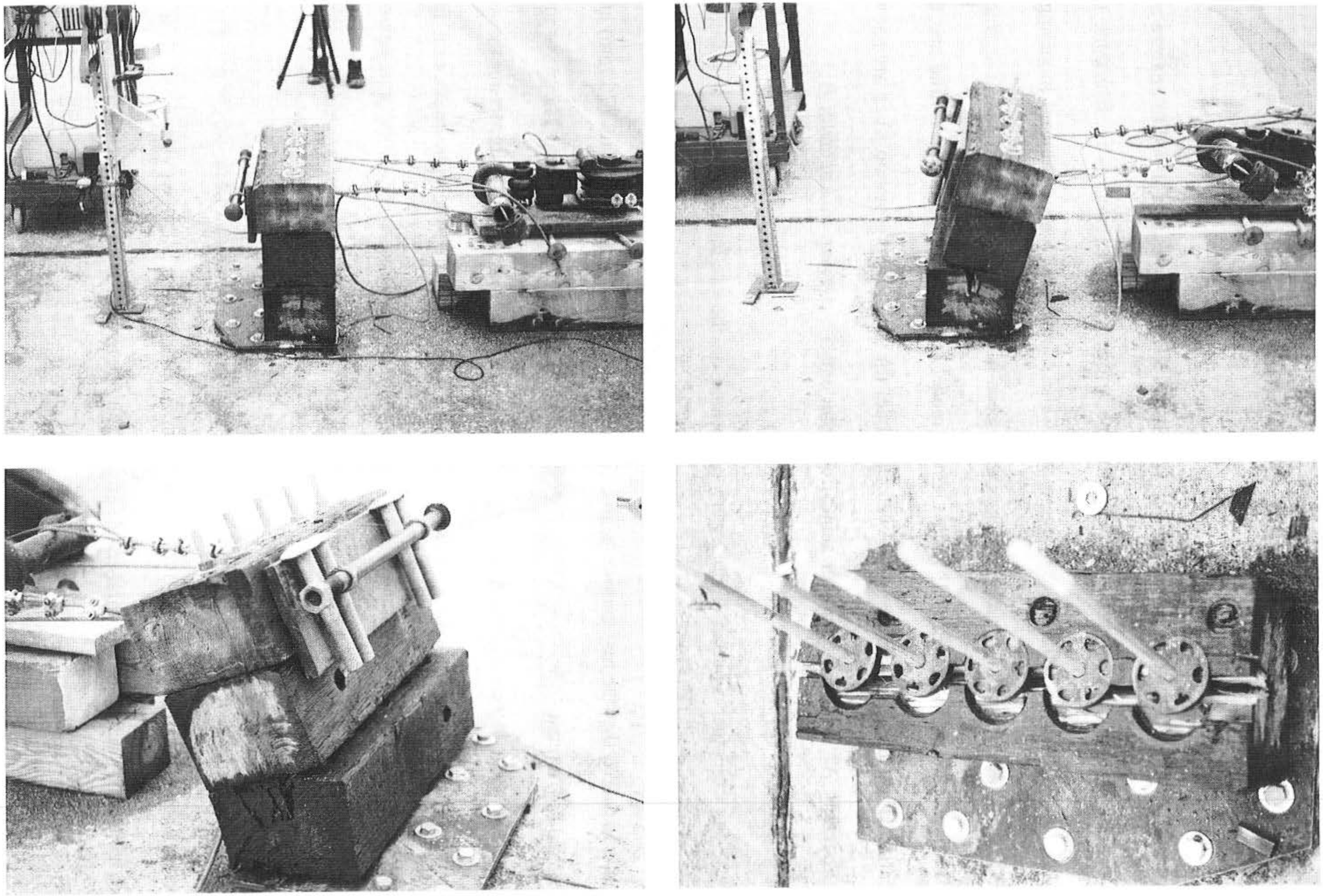

Figure 7. Test No. 3 Configuration and Deflected Position

6 COMPUTER SIMULATION MODELING - PHASE I

6.1 Background

Computer simulation modeling with BARRIER VII (18), was performed to analyze and predict the dynamic performance of the curb-type bridge railing as well as to determine the critical impact point (CIP) for the bridge railing. The simulations were conducted modeling a 2,000-kg (4,409-lb) pickup truck impacting at a speed of 50 km/h (31.1 mph) and at an angle of 25 degrees. The BARRIER VII finite element model of the curb-type bridge railing and the idealized finite element, 2-dimensional vehicle model for the 2,000-kg pickup truck are shown in Appendix A. A typical computer simulation input datafile is given in Appendix B.

6.2 BARRIER VII Results

Six computer simulation runs were performed on the preliminary design at different impact locations. The impact location and results for each simulation are shown in Table 3. The results indicated that the maximum dynamic deflection was approximately 3.0 in. (76 mm) and occurred approximately 75 in. (1905 mm) downstream from the impact location. The maximum lateral post shear force was 10.5 kips (46.7 kN) and occurred from a vehicle impacting the rail 75 in. (1905 mm) upstream from post no. 6, as shown in Figure A-1. The maximum rail bending moment was approximately 452 kip-in. (51.1 kN-m) and occurred from a vehicle impacting the rail 60 in. (1524 mm) upstream from the midspan rail location between post nos. 5 and 6, as shown in Figure A-1.

The analysis of the simulation results indicated that the posts and deck attachment were over-designed by approximately 20 to 33%. Therefore, the Design No. 1 was modified at each post location by reducing the number of vertical bolts from five to four, reducing the number

Table 3. Computer Simulation Test Matrix and Results - Phase I

Test No.	Impact Node	Impact Point (in.)[1]	Maximum Post Shear Along B-Axis (kips)	Maximum Beam Moment About C-Axis (kip-in.)	Maximum Dynamic Rail Deflection (in.)
1	16	135	8.80 @ Node 25	441.31 @ Node 20	3.04 @ Node 21
2	17	120	9.58 @ Node 25	452.27 @ Node 21	3.03 @ Node 22
3	18	105	10.11 @ Node 25	436.32 @ Node 22	3.00 @ Node 23
4	19	90	10.41 @ Node 25	401.37 @ Node 23	2.96 @ Node 24
5	20	75	10.48 @ Node 25	350.48 @ Node 24	2.94 @ Node 25
6	21	60	10.30 @ Node 25	386.16 @ Node 27	2.95 @ Node 26

[1] - Longitudinal distance measured upstream from post no. 6 (node 25) (i.e., post spacing equal to 120 in.).

Post Parameters:

Stiffness k_B = 3.56 kips/in.
Yield Moment M_A = 279.73 kip-in.
Shear Failure Limit F_B = 20 kips
Deflection Limit Δ_B = 6 in.

Stiffness k_A = 10.00 kips/in.
Yield Moment M_B = 409.38 kip-in.
Shear Failure Limit F_A = 30 kips
Deflection Limit Δ_A = 1 in.

of horizontal lag screws from four to three, and decreasing the length of the scupper blocks from 28 to 23 in. (711 to 584 mm). In addition, the rail overhang distance on the traffic-side face was increased from 1 in. to 2¼ in. (25 to 57 mm) to prevent the vehicle's front wheel from snagging on the upstream face of the timber posts and to reduce the potential of the wheel contacting and climbing up the scupper blocks.

7 DEVELOPMENTAL TESTING - PHASE II

7.1 Static Testing

Following the analysis of the computer simulation results, design modifications were made to the Design No. 1, as discussed in Section 6.2. Static testing was again used to determine the force-deflection characteristics and the structural capacity of a four-bolt connection between the glulam rail, scupper blocks, and deck. The static testing apparatus was the same as that used during the Developmental Testing - Phase I. Three additional static tests were performed and are described below.

7.1.1 Test No. 4

Test no. 4 was conducted on a configuration consisting of a 6¾-in. (171-mm) high glulam rail supported by two scupper blocks - one 7½-in. (190-mm) high and one 5½-in. (140-mm) high., as shown in Figure 8. Four bolts were placed along the 23-in. (584-mm) long blocks using shear plates at all available locations. Photographs of the deflected configuration are also shown in Figure 8. The force-deflection curve for test no. 4 is provided in Figure 9. The maximum load applied to the system was 14,300 lbs (63,600 N) which corresponded with a rail deflection of 9.8 in. (249 mm), as measured at the top of the glulam rail. The load was then released, resulting in a permanent set of approximately 5.5 in. (140 mm). The rail deformations occurred due to rotations caused by the compaction of wood fibers in the compression regions, the formation of gaps betweens timber blocks in the tension regions, and a tension failure of the lower scupper block propagating from the bolt line, as shown in Figure 8.

7.1.2 Test No. 5

Test no. 5, as shown in Figure 10, was conducted on the same configuration as used for

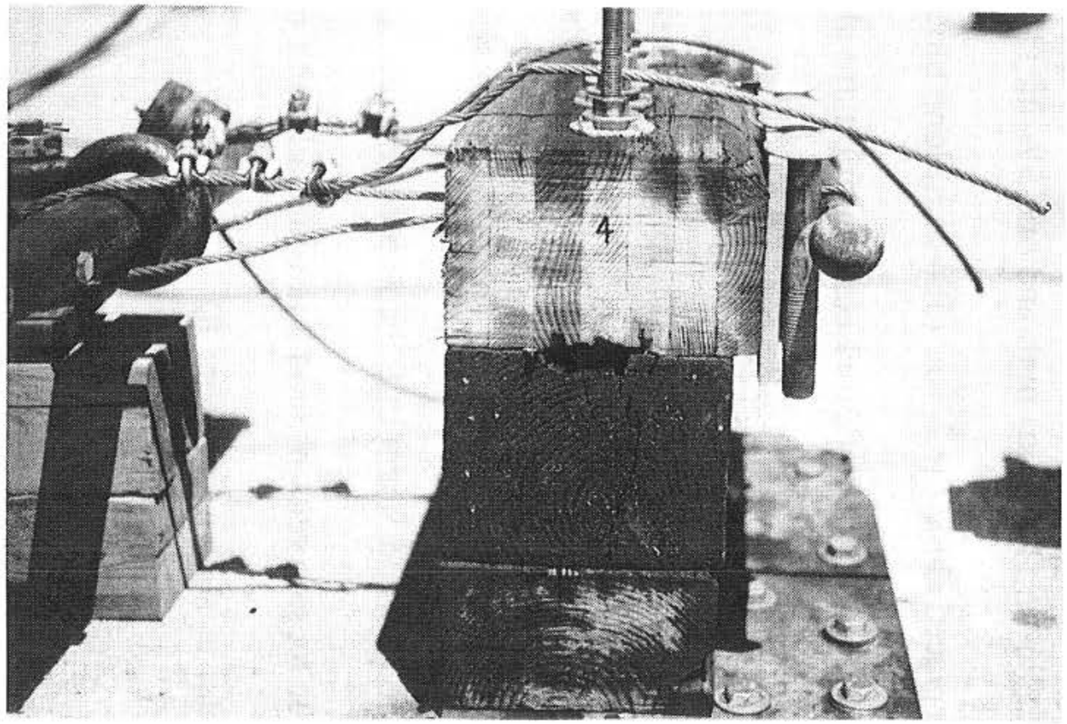

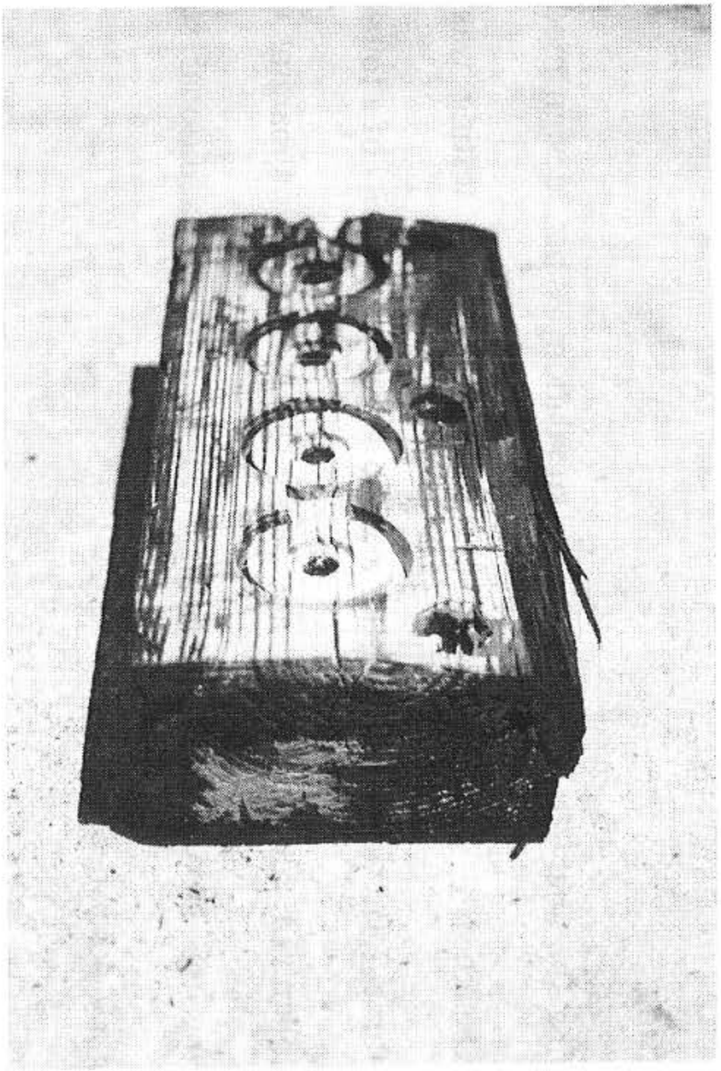

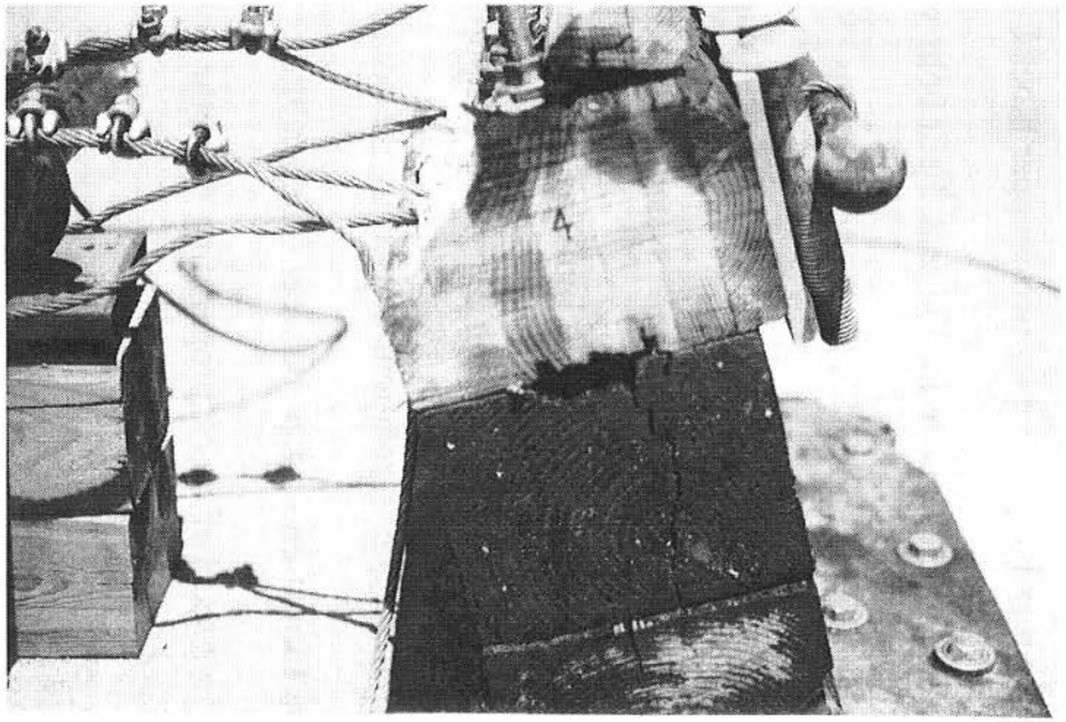

Figure 8. Test No. 4 Configuration and Deflected Position

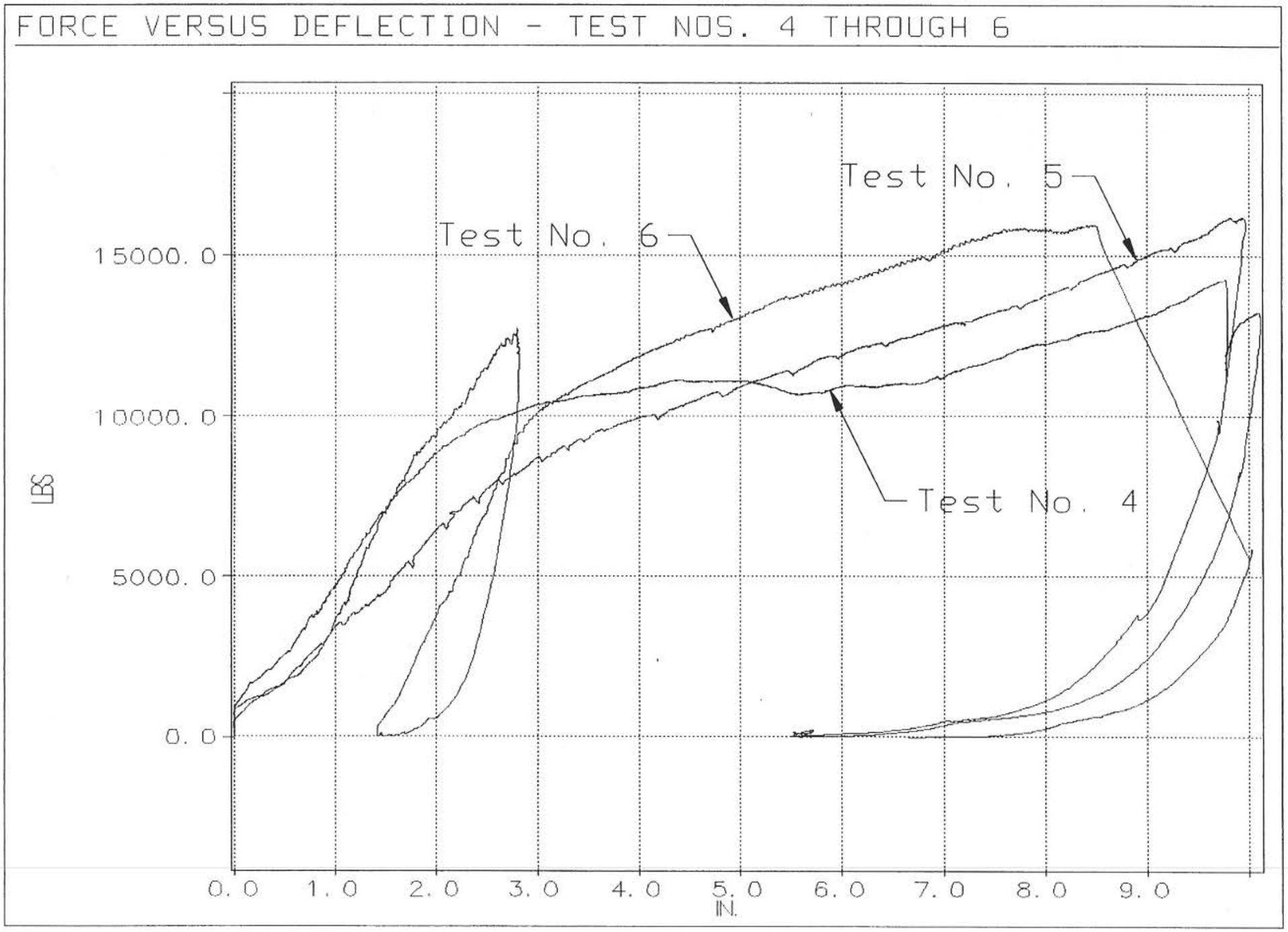

Figure 9. Force-Deflection Curves for Test Nos. 4, 5, and 6

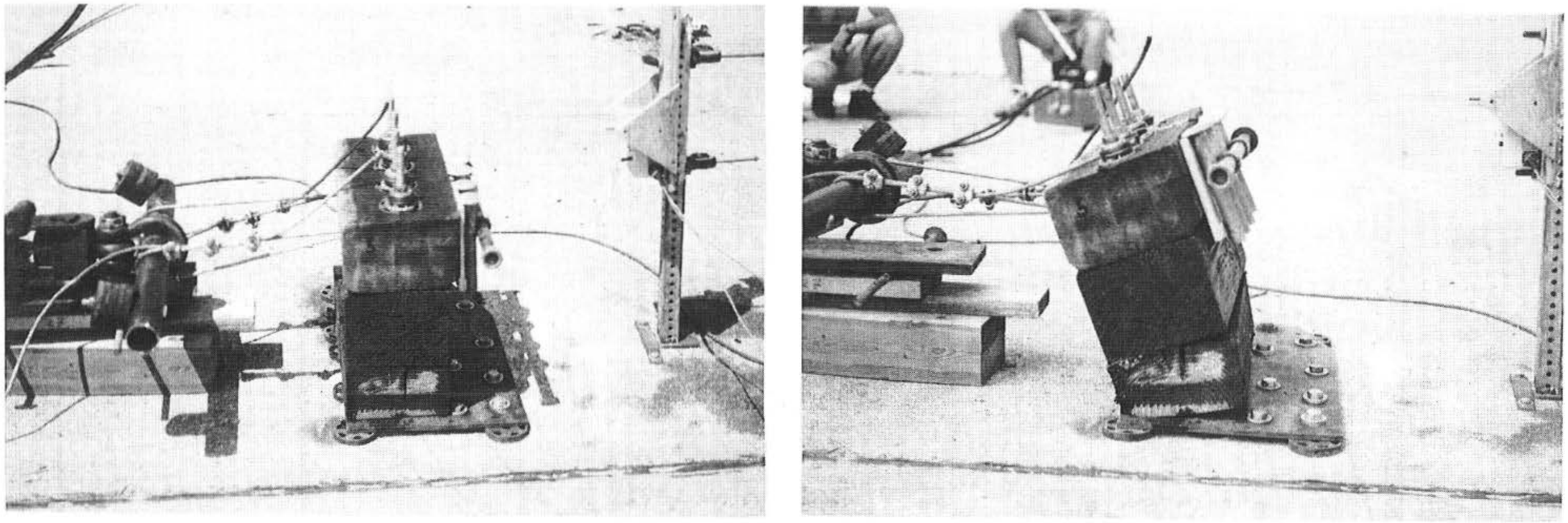

Figure 10. Test No. 5 Configuration and Deflected Position

test no. 4, except that no shear plates were used at any timber surface. Photographs of the deflected configuration are also shown in Figure 10. The force-deflection curve for test no. 5 is provided in Figure 9. The maximum load applied to the system was 16,200 lbs (72,100 N) which corresponded with a rail deflection of 9.8 in. (249 mm), as measured at the top of the glulam rail. The load was then released, resulting in a permanent set of approximately 5.5 in. (140 mm). The rail deformations occurred due to rotations caused by the compaction of wood fibers in the compression regions, the formation of gaps betweens timber blocks in the tension regions, and a tension failure of the lower scupper block propagating from the bolt line, as shown in Figure 10.

7.1.3 Test No. 6

Test no. 6, as shown in Figure 11, was conducted on the same configuration as used for test no. 5, except that shear plates were used on the bottom surface of the lower scupper block. Photographs of the deflected configuration are also shown in Figure 11. The force-deflection curve for test no. 6 is provided in Figure 9. During the test, it was discovered that the cable and pulley assembly were not properly aligned, and the test was stopped. After releasing the load to repair the cable and pulley assembly, the test was continued. The maximum load applied to the system was 15,900 lbs (70,700 N) which corresponded with a rail deflection of 8.5 in. (216 mm), as measured at the top of the glulam rail. It is noted that the maximum load was measured at the time that the glulam rail fractured, as shown in Figure 11. The rail deformations occurred due to rotations caused by the compaction of wood fibers in the compression regions, the formation of gaps between the timber blocks in the tension regions, and a tension failure of the lower scupper block propagating from the bolt line, as shown in Figure 11.

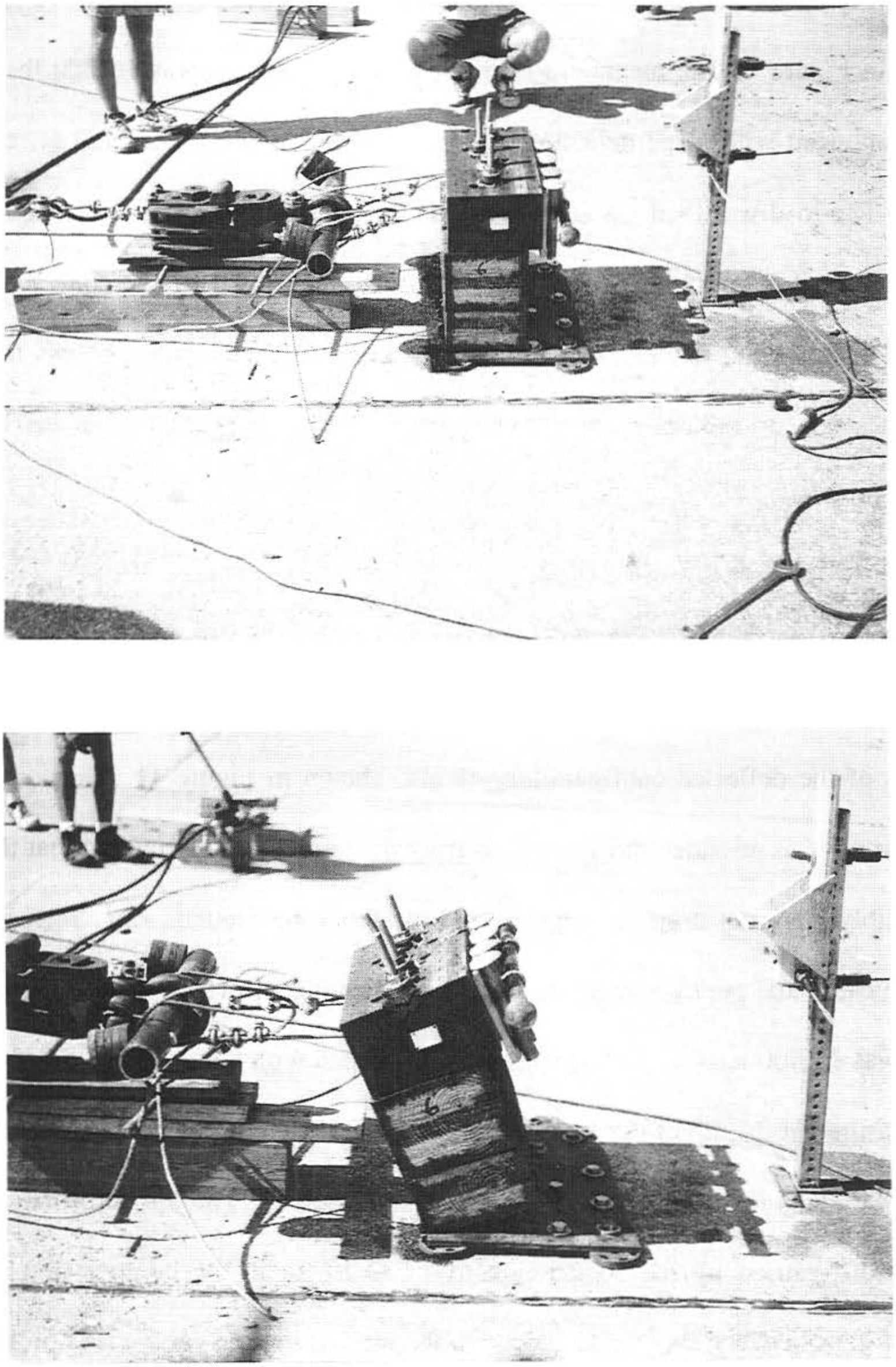

Figure 11. Test No. 6 Configuration and Deflected Position

8 COMPUTER SIMULATION MODELING - PHASE II

8.1 Design Modifications

Following the Developmental Testing - Phase II, it was determined that the four-bolt attachment between the glulam rail, scupper blocks, and deck could provide adequate structural capacity without damaging the bridge deck. Therefore, computer simulation modeling was again used to analyze and predict the dynamic performance of the bridge railing as well as to determine the CIP.

8.2 BARRIER VII Results

Six additional computer simulation runs were performed on the four-bolt design at different impact locations. The impact location and results for each simulation are shown in Table 4. The results indicated that the maximum dynamic deflection was approximately 2.8 in. (71 mm) and occurred approximately 75 in. (1905 mm) downstream from the impact location. The maximum lateral post shear force was 9.9 kips (44.0 kN) and occurred from a vehicle impacting the rail 75 to 90 in. (1905 to 2286 mm) upstream from post no. 6, as shown in Figure A-1. The maximum rail bending moment was approximately 431 kip-in. (48.7 kN-m) and occurred from a vehicle impacting the rail 60 in. (1524 mm) upstream from the midspan rail location between post nos. 5 and 6, as shown in Figure A-1.

The analysis of the simulation results indicated that the curb-type bridge railing with a four-bolt attachment between the glulam rail, scupper blocks, and deck could withstand the impact resulting from a 2,000-kg (4,409-lb) pickup truck impacting at a speed of 50 km/hr (31.1 mph) and an angle of 25 degrees.

Table 4. Computer Simulation Test Matrix and Results - Phase II

Test No.	Impact Node	Impact Point (in.)[1]	Maximum Post Shear Along B-Axis (kips)	Maximum Beam Moment About C-Axis (kip-in.)	Maximum Dynamic Rail Deflection (in.)
7	16	135	9.61 @ Node 25	423.56 @ Node 20	2.65 @ Node 21
8	17	120	9.79 @ Node 25	431.43 @ Node 21	2.65 @ Node 22
9	18	105	9.81 @ Node 25	420.64 @ Node 22	2.67 @ Node 23
10	19	90	9.85 @ Node 25	394.72 @ Node 23	2.71 @ Node 24
11	20	75	9.85 @ Node 25	353.00 @ Node 24	2.75 @ Node 25
12	21	60	9.81 @ Node 25	377.55 @ Node 27	2.76 @ Node 26

[1] - Longitudinal distance measured upstream from post no. 6 (node 25) (i.e., post spacing equal to 120 in.).

Post Parameters:

Stiffness k_B = 4.53 kips/in.
Yield Moment M_A = 178.13 kip-in.
Shear Failure Limit F_B = 15 kips
Deflection Limit Δ_B = 6.5 in.

Stiffness k_A = 10.00 kips/in.
Yield Moment M_B = 409.38 kip-in.
Shear Failure Limit F_A = 30 kips
Deflection Limit Δ_A = 1 in.

9 DESIGN NO. 2 DETAILS

9.1 Timber Deck and Substructure

A full-size simulated timber bridge system was constructed at the MwRSF. In order to simulate an actual timber bridge installation, the longitudinal glulam timber bridge deck was mounted on six reinforced-concrete bridge supports. The inner three concrete bridge supports had center-to-center spacings of 5.72 m (18 ft 9 in.) whereas the outer two spacings were 5.56 m (18 ft 3 in.).

The longitudinal glulam timber deck consisted of ten rectangular panels. The panels measured 1.22-m (3-ft 11⅞-in.) wide by 5.70 m (18-ft 8½-in.) long by 273-mm (10¾-in) thick. The timber deck was constructed so that two panels formed the width of the deck and five panels formed the length of the deck. The longitudinal glulam timber deck was fabricated with West Coast Douglas Fir and treated with pentachlorophenol in heavy oil to a minimum net retention of 0.6 lbs/ft^3 (9.61 kg/m^3) as specified in AWPA Standard C14 (19). At each longitudinal midspan location of the timber deck panels, stiffener beams were bolted transversely across the bottom side of the timber deck panels per AASHTO bridge design requirements. The stiffener beams measured 130-mm (5⅛-in.) wide by 152-mm (6-in.) thick by 2.44-m (8-ft) long. In addition, a 2-in. (51-mm) asphalt wearing surface was placed on the top of the timber deck in order to represent actual field conditions.

9.2 Glulam Timber Curb Bridge Railing System

The total length of the test installation was 100 ft (30.48 m), as shown in Figures 12 through 14. The curb-type bridge railing consisted of three major structural components: (1) a longitudinal glulam timber rail; (2) sawn lumber scupper blocks; and (3) steel splice plates.

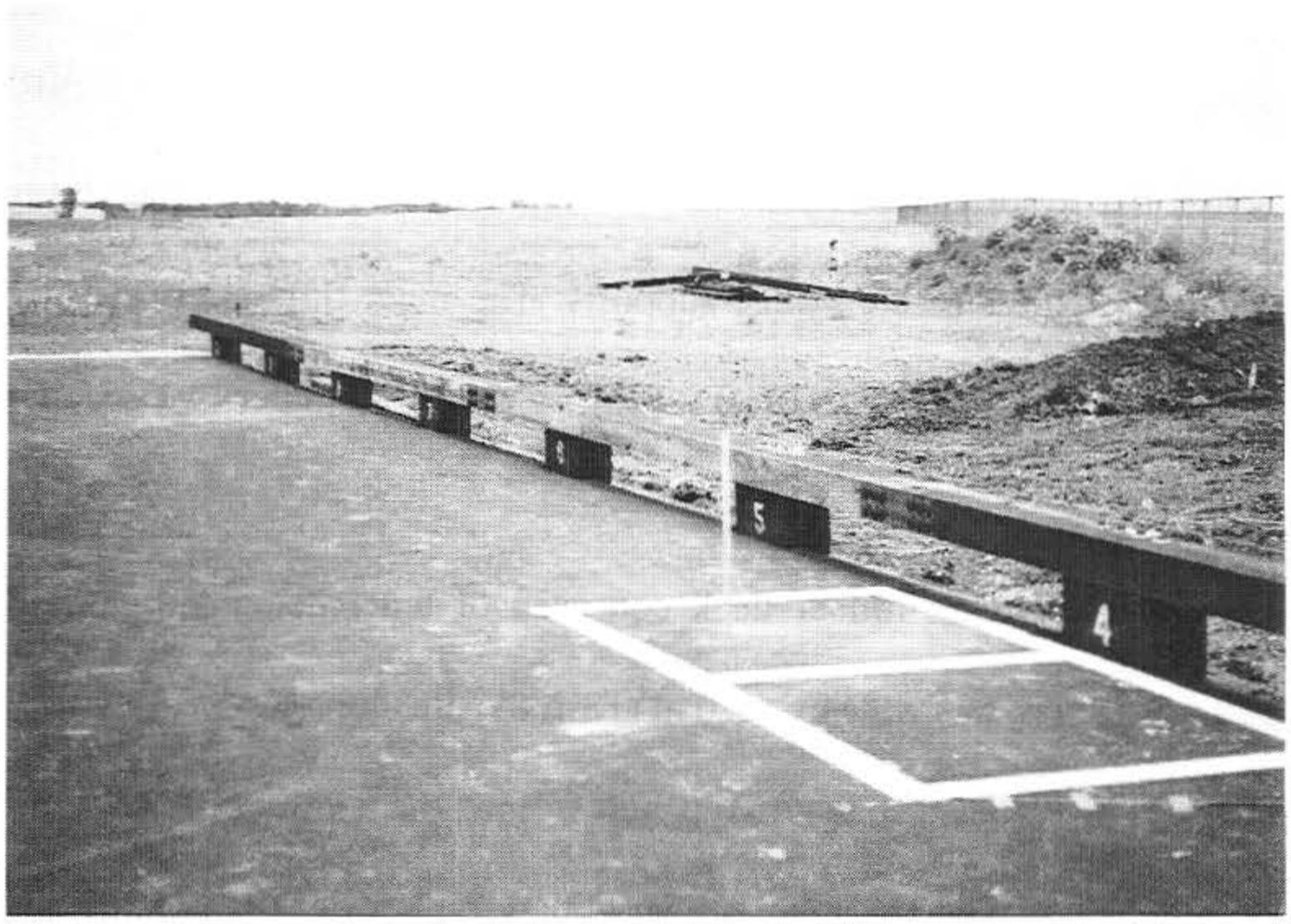

Figure 12. Curb-Type Bridge Railing System

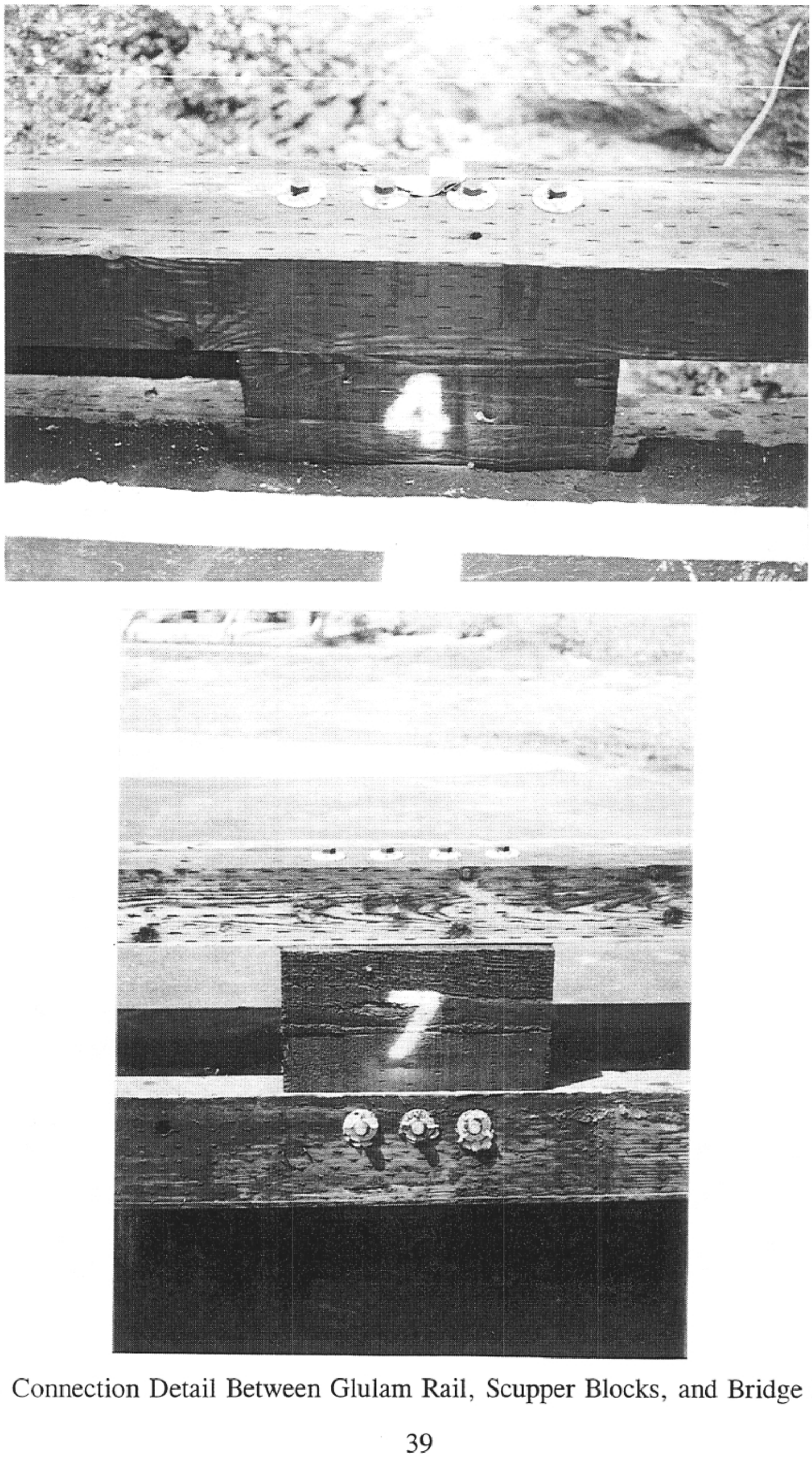

Figure 13. Connection Detail Between Glulam Rail, Scupper Blocks, and Bridge Deck

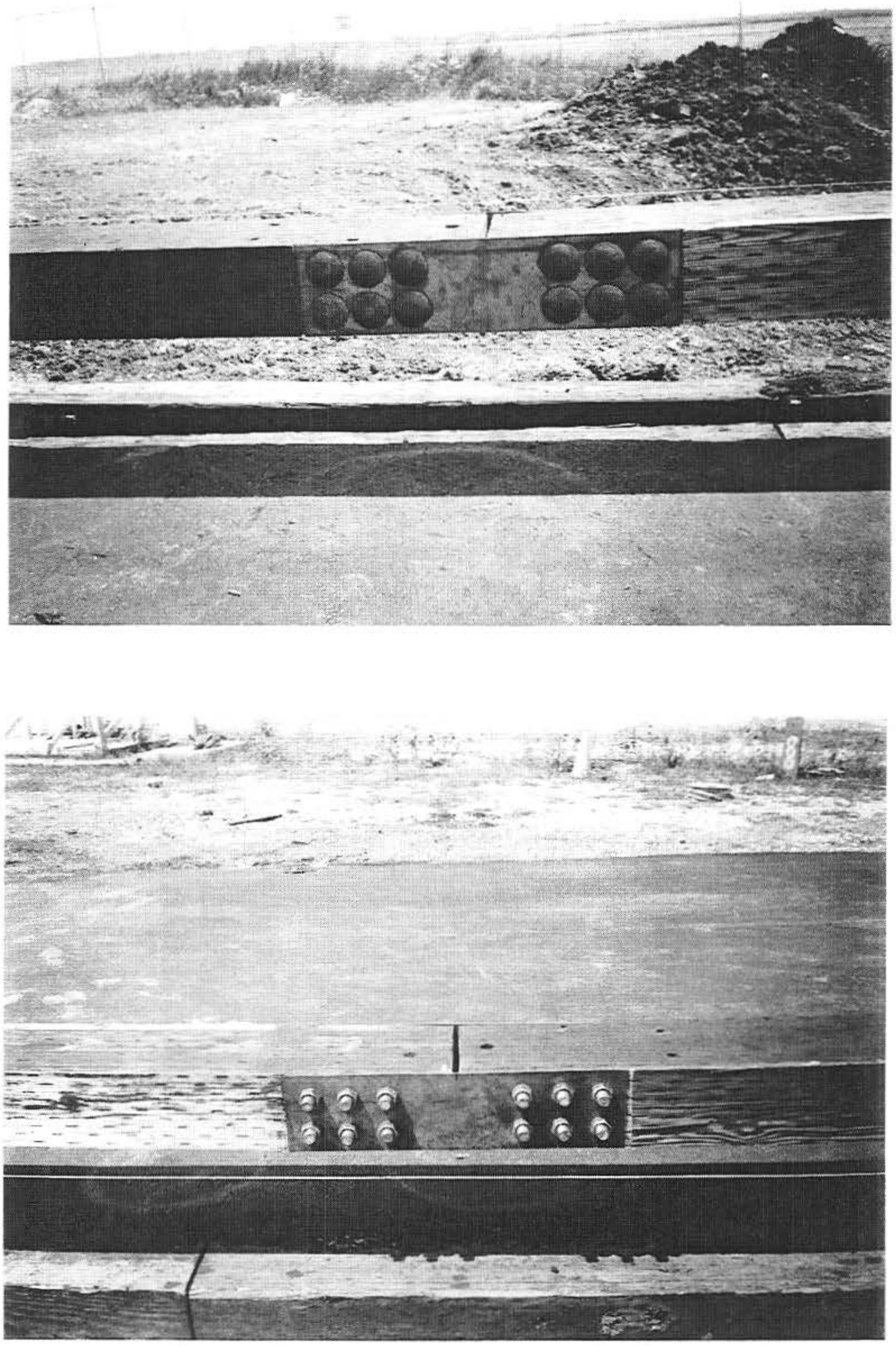

Figure 14. Steel Splice Plate Connection for Glulam Rail

Detailed drawings of the bridge rail components are provided in Figure 15.

The bridge railing system incorporated five 19-ft 11½-in. (6083 mm) long timber glulam rail sections supported by ten timber scupper blocks spaced on 10-ft (3048-mm) centers. The glulam rail was fabricated from Combination No. 2 West Coast Douglas Fir and treated in the same manner as the timber deck. The glulam rail was 6¾-in. (171-mm) deep by 10½-in. (267-mm) wide. The top mounting height of the glulam rail was 17¾ in. (451-mm) above the asphalt wearing surface.

The scupper blocks were fabricated from S4S No. 1 Grade Douglas Fir and treated to meet AWPA Standard C14 with 12 lbs/ft^3 (192.22 kg/m^3) creosote (19). Two 23-in. (584-mm) long scupper blocks, one measuring 5½-in. (140-mm) high by 9½-in. (241-mm) wide and one 7½-in. (190-mm) high by 9½-in. (241-mm) wide, were used at each post location. Four ¾-in. (19-mm) diameter by 33-in. (838-mm) long ASTM A307 galvanized hex head bolts, in conjunction with 4-in. (102-mm) diameter split rings and ¾-in. (19-mm) malleable iron washers, were used to attach the glulam rail and scupper blocks to the surface of the bridge deck. Three ¾-in. (19-mm) diameter by 12-in. (305-mm) long ASTM A307 galvanized lag screws were placed in the outer vertical face of the bridge deck at each post location to prevent delamination of the longitudinal timber deck panels. The lag screws were located 3-in. from the top of the bridge deck and were predrilled according to the specifications shown on Figure 15.

The glulam rail sections were spliced together with 3/16-in. (4.8-mm) thick ASTM A572 grade 42 steel plates on the traffic- and back-side faces of the glulam rail using twelve 1-in. (25-mm) diameter by 12-in. (305-mm) long ASTM A307 galvanized dome head bolts.

General Configuration

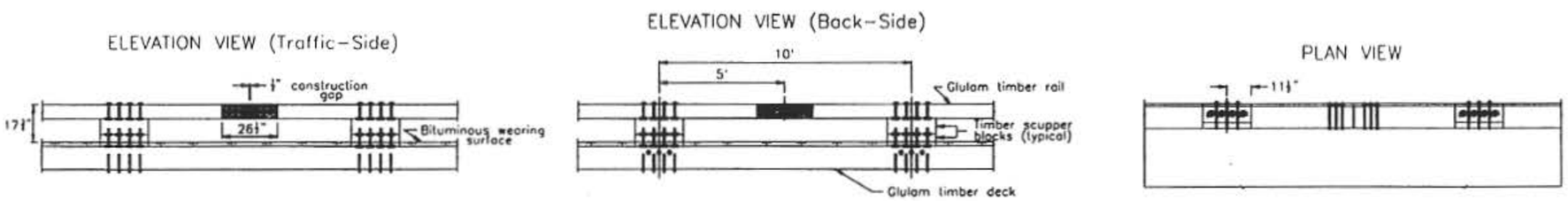

Pre-Assembly Timber Modifications

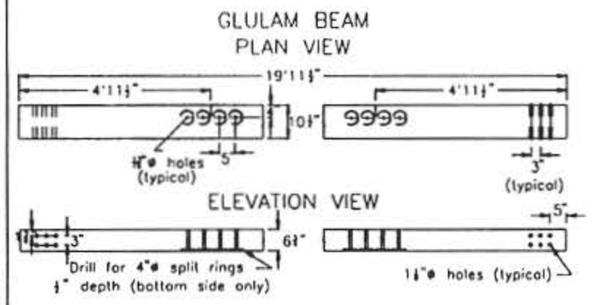

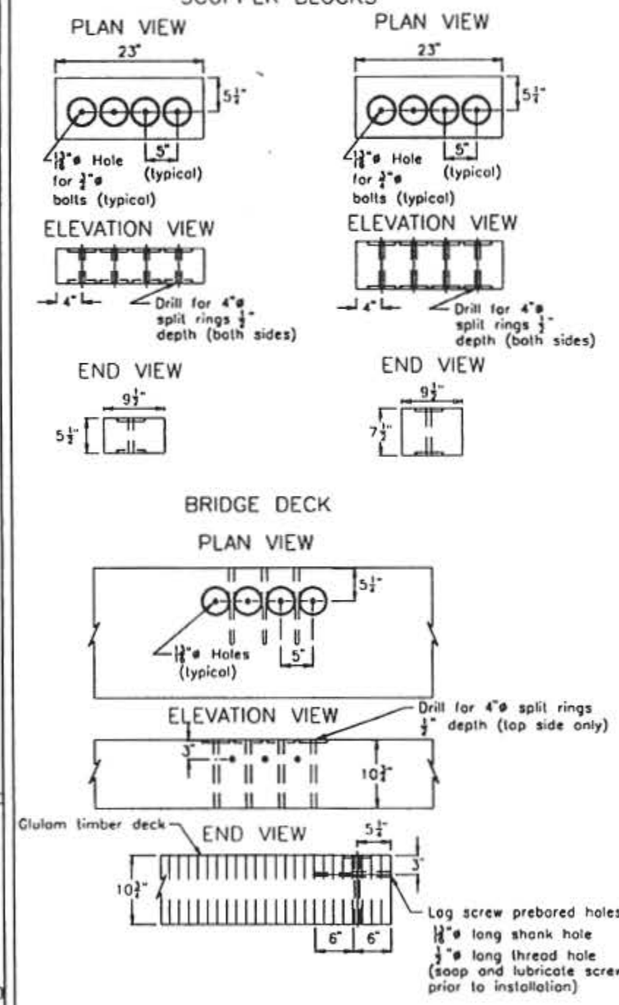

A

Railing Details

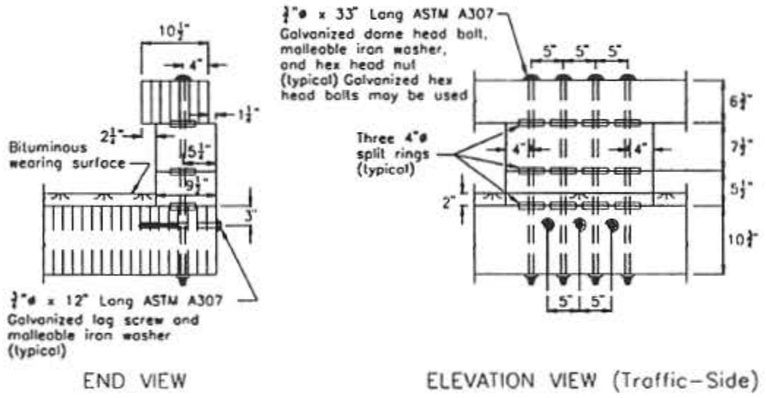

B

Splice Details

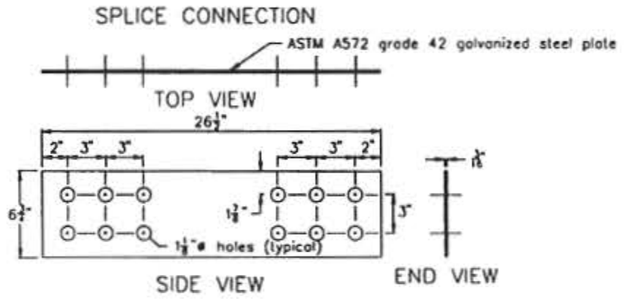

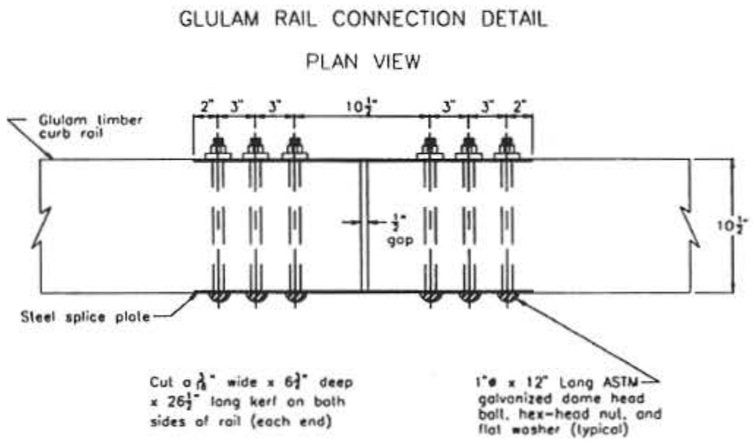

C

Typical Bridge-Rail Layout (100 ft.)

NCHRP 350 Test Level 1 (TL-1)
Timber Curb - Type
Bridge Railing System for
Low - Volume Roads

Figure 15. Bridge Rail Design Details (Design No. 2)

10 TEST CONDITIONS

10.1 Test Facility

The testing facility is located at the Lincoln Air-Park on the NW end of the Lincoln Municipal Airport and is approximately 5 mi (8.0 km) NW of the University of Nebraska-Lincoln. The site is protected by an 8-ft (2.44-m) high chain-link security fence.

10.2 Vehicle Tow and Guidance System

A reverse cable tow system with a 1:2 mechanical advantage was used to propel the test vehicles. The distance traveled and the speed of the tow vehicle are one-half that of the test vehicle. The test vehicle was released from the tow cable before impact with the bridge rail. A fifth wheel, built by the Nucleus Corporation, was located on the tow vehicle and used in conjunction with a digital speedometer to increase the accuracy of the test vehicle impact speed.

A vehicle guidance system developed by Hinch (20) was used to steer the test vehicle. A guide-flag, attached to the front-left wheel and the guide cable, was sheared off before impact. The 3/8-in. (9.5-mm) diameter guide cable was tensioned to approximately 3,000 lbs (13.3 kN), and supported laterally and vertically every 100 ft (30.48 m) by hinged stanchions. The hinged stanchions stood upright while holding up the guide cable, but as the vehicle was towed down the line, the guide-flag struck and knocked each stanchion to the ground. The vehicle guidance system was approximately 400-ft (122-m) long.

10.3 Test Vehicle

A 1985 Ford F-250 ¾-ton pickup truck was used as the test vehicle. The test inertial and gross static weights were 4,435 lbs (2,012-kg). The test vehicle is shown in Figure 16 and vehicle dimensions are shown in Figure 17.

Figure 16. Test Vehicle, Test CTBR-1

Date: 6/23/95 Test Number: CTBR-1 Model: F250

Make: Ford Vehicle I.D.#: 1FTEF25Y9EPA99219

Tire Size: LT215/85 R16 Year: 1984 Odometer: 51960

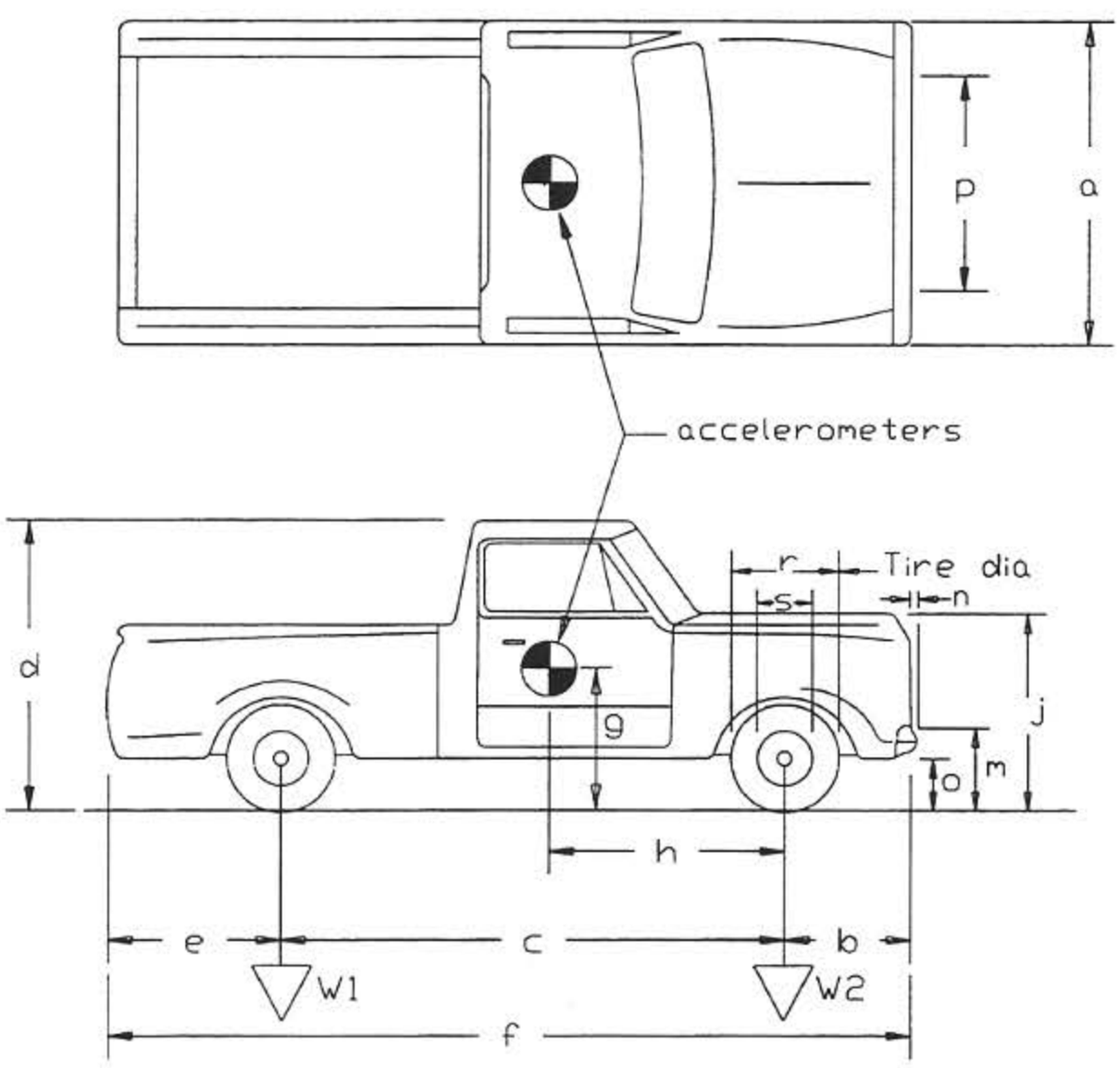

Vehicle Geometry - in

a	74"	b	28"
c	133.5"	d	71.5"
e	51.5"	f	213"
g	28.75"	h	60"
i	---	j	49.5"
k	---	l	---
m	26.0"	n	1"
o	16.75"	p	65"
r	29.25"	s	17.5"

Engine Type 6 cyl.

Engine Size 300 cubic in.

Transmission Type:

Automatic or (Manual)

FWD or (RWD) or 4WD

Weight - lbs	Curb	Test Inertial	Gross Static
W_1 (rear)	1695	1919	1919
W_2 (front)	2415	2516	2516
W_T (total)	4110	4435	4435

Note any damage prior to test: minor dents in left-side door.

Figure 17. Vehicle Dimensions, Test CTBR-1

The Elevated Axle Method (21) was used to determine the vertical component of the center of gravity. This method converts measured wheel weights at different elevations to the location of the vertical component of the center of gravity. The longitudinal component of the center of gravity was determined using the measured axle weights. The location of the final center of gravity is shown in Figure 17. Vehicle ballast, consisting of steel plates, was rigidly attached to the floor of the pickup truck box and used to obtain the desired weight.

Five square, black and white-checkered targets were placed on the vehicle to aid in the analysis of the high-speed film, as shown in Figures 16 and 18. One target was placed on the center of gravity at the driver's side of the vehicle. The remaining targets were located for reference so that they could be viewed from the high-speed cameras.

The front wheels of the test vehicle were aligned for camber, caster, and toe-in values of zero so that the vehicles would track properly along the guide cable. Two 5B flash bulbs were mounted on the hood of the vehicles to pinpoint the time of impact with the bridge railing on the high-speed film. The flash bulbs were fired by a pressure tape switch mounted on the front face of the bumper. A remote controlled brake system was installed in the test vehicle so the vehicle could be brought safely to a stop after the test.

10.4 Data Acquisition Systems

10.4.1 Accelerometers

Two triaxial piezoresistive accelerometer systems with a range of $\pm$200 g's (Endevco Model 7264) were used to measure the acceleration in the longitudinal, lateral, and vertical directions. Two accelerometers were mounted in each of the three directions and were rigidly attached to a metal block mounted at the center of gravity. Accelerometer signals were received

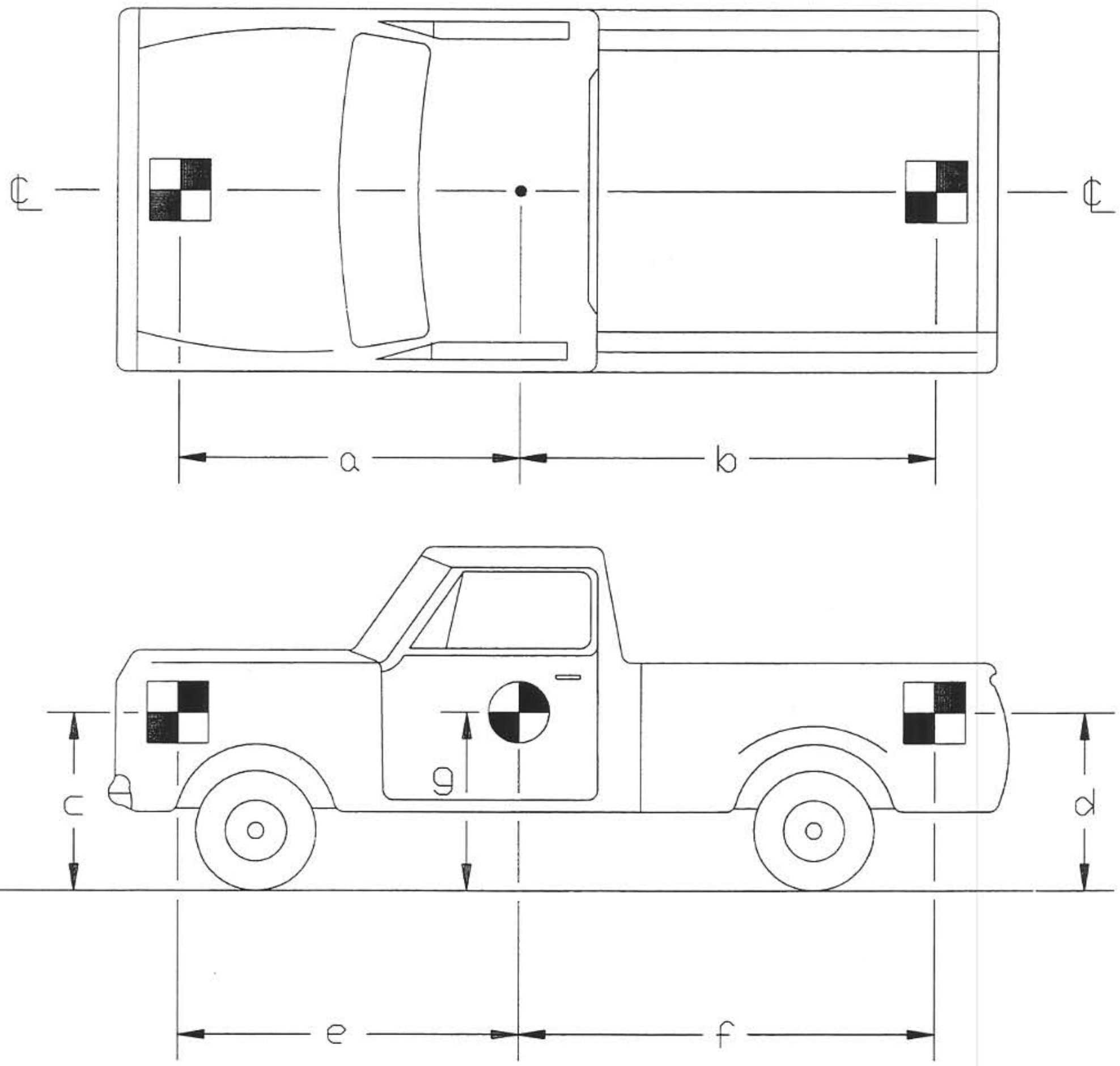

TEST #: CTBR-1

TARGET GEOMETRY
INCHES

a	57.87	c	41	e	57.87	g	28
b	96	d	41	f	96		

Figure 18. Vehicle Target Locations, Test CTBR-1

and conditioned by an onboard Series 300 Multiplexed FM Data System built by Metraplex Corporation. The multiplexed signal was then transmitted to the Honeywell 101 Analog Tape Recorder. Computer software, "EGAA" and "DADiSP" were used to digitize, analyze, and plot the accelerometer data.

A backup triaxial piezoresistive accelerometer system with a range of $\pm$200 G's was also used to measure the acceleration in the longitudinal, lateral, and vertical directions at a sample rate of 3,200 Hz. The environmental shock and vibration sensor/recorder system, Model EDR-3, was developed by Instrumented Sensor Technology (IST) of Okemos, Michigan. The EDR-3 was configured with 256 Kb of RAM memory and a 1,120 Hz filter. Computer software, "DynaMax 1 (DM-1)" and "DADiSP" were used to digitize, analyze, and plot the accelerometer data.

10.4.2 Rate Transducer

A Humphrey 3-axis rate transducer with a range of 250 deg/sec in each of the three directions (pitch, roll, and yaw) was used to measure the rates of motion of the test vehicle. The rate transducer was rigidly attached to the vehicles near the center of gravity of the test vehicle. Rate transducer signals were received and conditioned by an onboard Series 300 Multiplexed FM Data System built by Metraplex Corporation. The multiplexed signal was then transmitted by radio telemetry to a Honeywell 101 Analog Tape Recorder. Computer software, "EGAA" and "DADiSP" were used to digitize, analyze, and plot the rate transducer data.

10.4.3 High-Speed Photography

Five high-speed 16-mm cameras, with operating speeds of approximately 500 frames/sec, were used to film the crash test. A Red Lake Locam with a wide-angle 12.5-mm lens was placed above the test installation to provide a field of view perpendicular to the ground. A Red Lake

Locam with a 76-mm lens was placed downstream from the impact point and had a field of view parallel to the bridge rail. A Photec IV with an 55-mm lens was placed on thė traffic side of the bridge rail and had a field of view perpendicular to the bridge rail. A Red Lake Locam, with a 25-mm lens, was placed upstream from the impact point and had a field of view parallel to the bridge rail. A Red Lake Locam with a zoom lens was placed downstream and behind the bridge rail. A schematic of all five camera locations for test CTBR-1 is shown in Figures 19. In addition, a Bolex camera, with an operating speed of approximately 64 frames/sec, was used as a documentary camera.

A 10-ft (3.05-m) long by 5-ft (1.52-m) wide, white-colored grid was painted on the asphalt surface on the traffic side of the bridge rail. This grid was incremented in 5-ft (1.52-m) divisions to provide a visible reference system for use in the analysis of the overhead high-speed film. The film was analyzed using the Vanguard Motion Analyzer. Actual camera speed and camera divergence factors were considered in the analysis of the high-speed film.

10.4.4 Pressure Tape Switches

Five pressure-activated tape switches, spaced at 5-ft (1.52-m) intervals, were used to determine the speed of the vehicle before impact. Each tape switch fired a strobe light which sent an electronic timing signal to the data acquisition system as the left front tire of the test vehicle passed over it. Test vehicle speeds were determined from electronic timing mark data recorded on "EGAA" software. Strobe lights and high-speed film analysis are used only as a backup in the event that vehicle speeds cannot be determined from the electronic data.

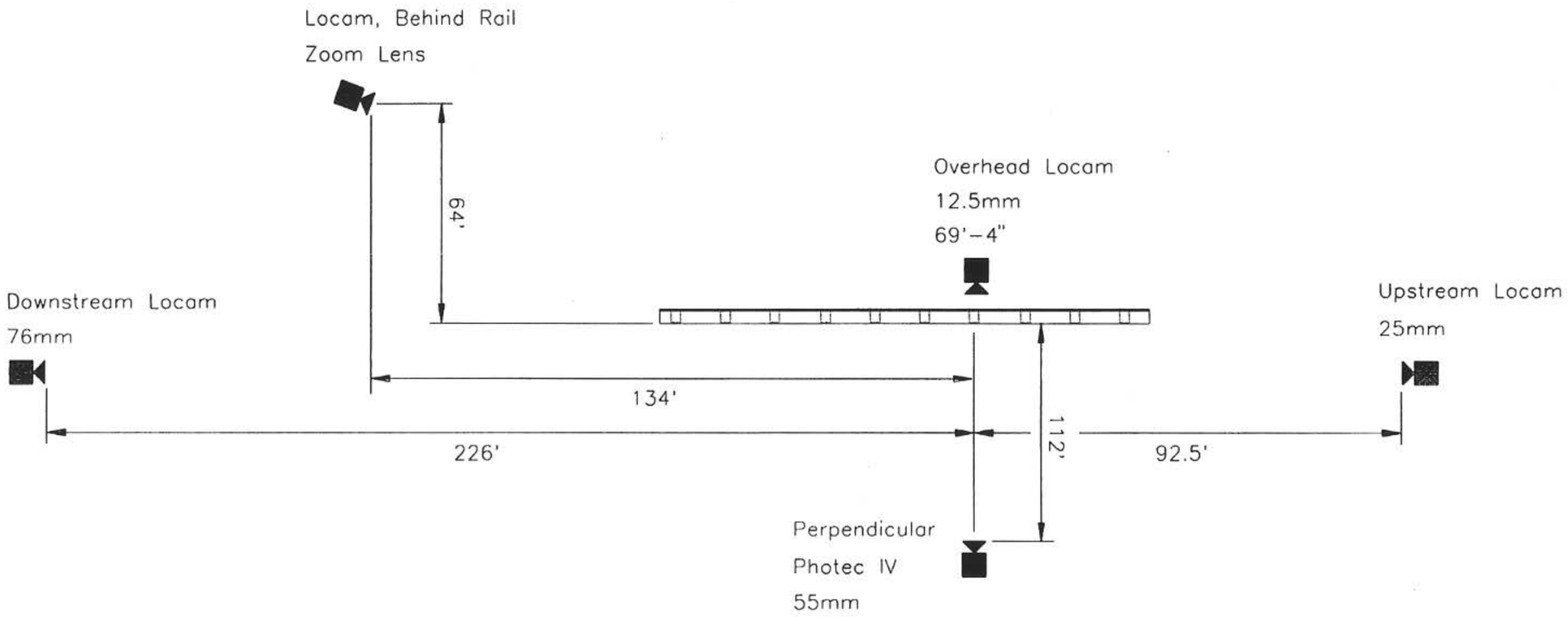

Figure 19. Location of High-Speed Cameras, Test CTBR-1

11 FULL-SCALE CRASH TEST

11.1 Test CTBR-1 (4,435 lbs (2,012 kg), 31.6 mph (50.9 km/hr), 24.3 degrees)

The pickup truck impacted the curb-type bridge railing at the center of post no. 4 and approximately 35 ft (10.67 m) from the upstream end of the bridge rail, as shown in Figure 20. A summary of the test results and the sequential photographs is presented in Figure 21. Additional sequential photographs are shown in Figures 22 and 23. Documentary photographs of the crash test are shown in Figures 24 through 26.

11.2 Test Description

During the initial impact with the bridge rail, the right-front tire was deformed, allowing the steel rim to gouge into the traffic-side face of the glulam rail. Subsequently, the tire continued to rotate and climb up the face of the rail and lost contact with the deck surface at 0.026 sec. At 0.119 sec, the right-front tire blew out due to contact with the glulam rail. From the overhead high-speed film, the maximum dynamic lateral deflection of 2.7 in. (69 mm) was observed at post no. 4 at 0.124 sec. The right-front tire was at the midspan between post nos. 4 and 5 at 0.144 sec. At 0.171 sec, the right-front tire was positioned on the top of the glulam rail with front tires turned toward the bridge rail. The left-front and right-rear tires lost contact with the deck surface at 0.181 sec and 0.231 sec, respectively. At 0.241 sec, the right-front tire became airborne, leaving the top of the glulam rail. The right-rear tire impacted the bridge rail at 0.353 sec, causing the pickup truck to yaw counterclockwise away from the bridge rail. The pickup truck reached a maximum pitch angle at 0.422 sec. Subsequently, the pickup truck nearly became parallel to the bridge rail at 0.433 sec. At 0.539 sec, the left-rear tire lost contact with deck surface, and the right-front tire contacted the top of the glulam rail at 0.542 sec. At 0.723

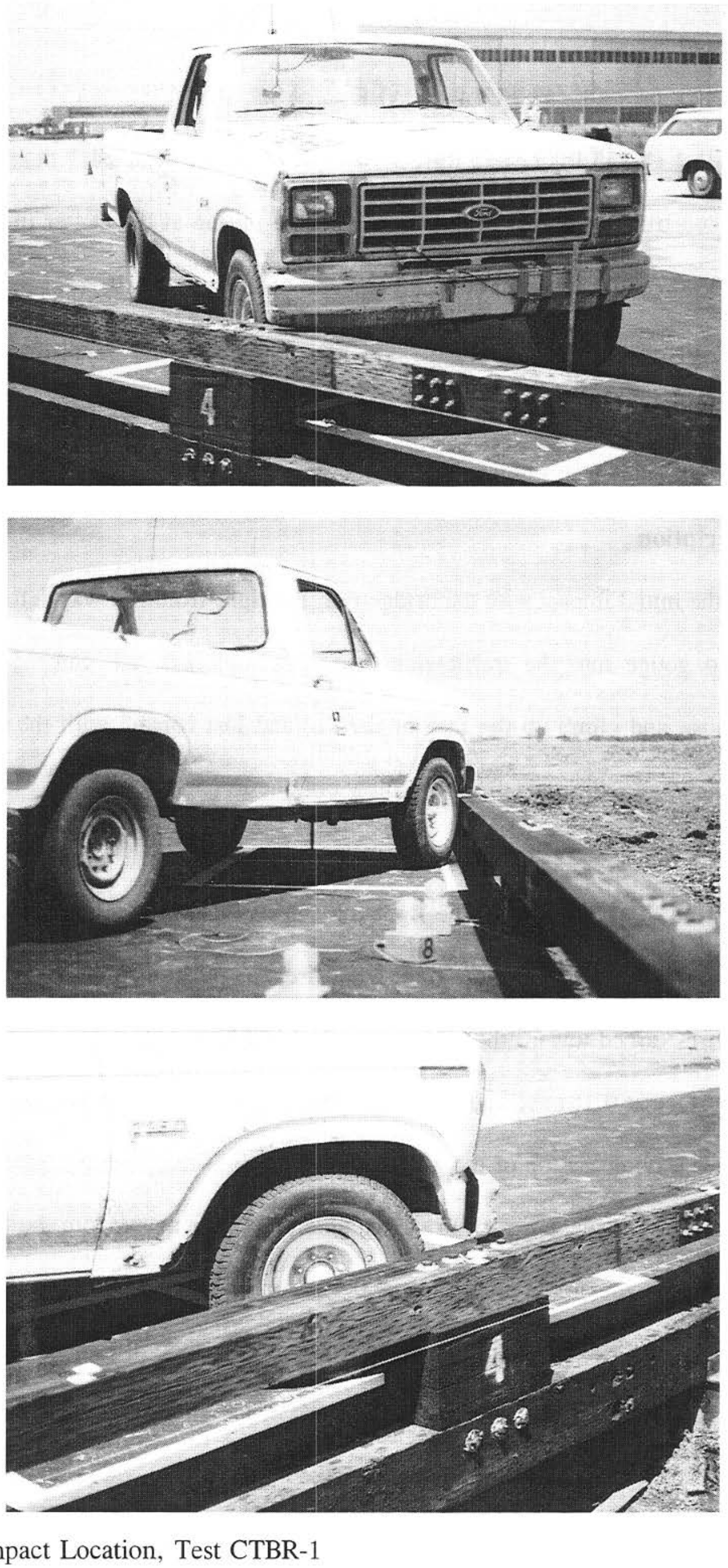

Figure 20. Impact Location, Test CTBR-1

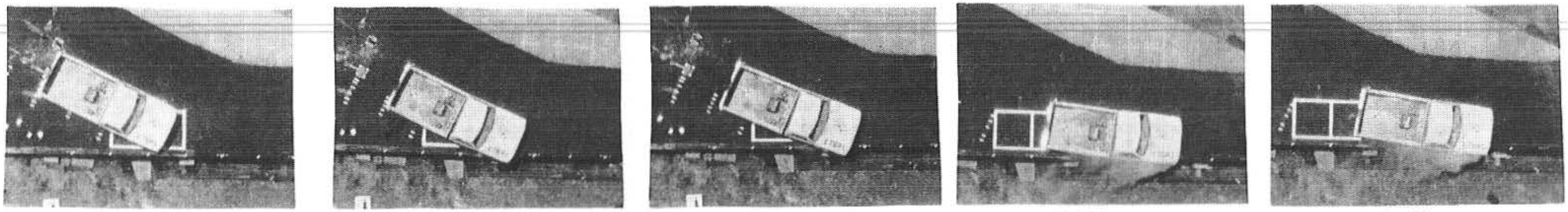

0.000 sec | 0.124 sec | 0.144 sec | 0.433 sec | 0.483 sec

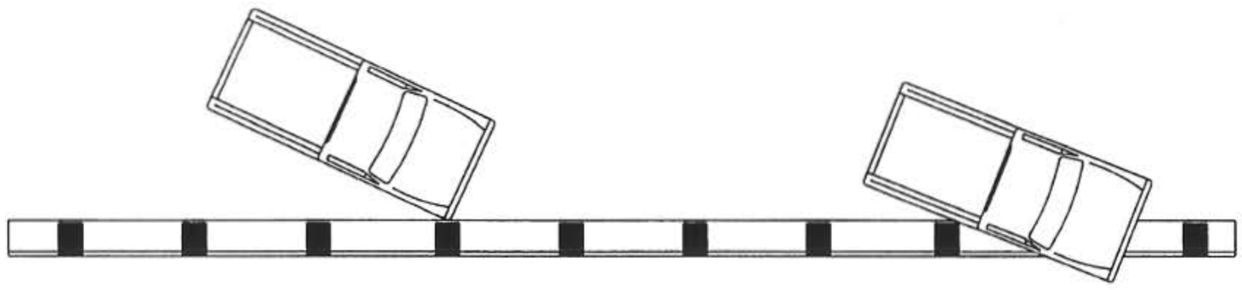

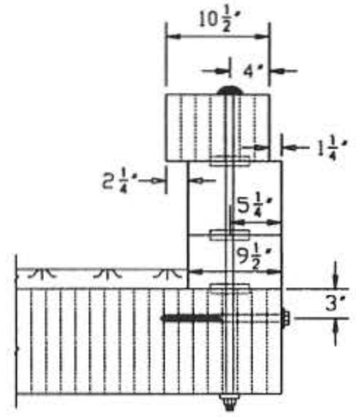

- Test Number CTBR-1
- Date 6/23/95
- Bridge Rail Installation . . . . . TL-1 Curb-Type Railing System
- Total Length . . . . . 100 ft
- Glulam Curb Rail
  - Size . . . . . 6¾ in. x 10½ in.
  - Top Mounting Height . . . . . 17¾ in.
  - Material . . . . . West Coast Douglas Fir
  - Grade . . . . . Combination No. 2
- Scupper Blocks
  - Size . . . . . 7½ in. x 9½ in. 23 in. & 5½ in. x 9½ in. 23 in.
  - Material . . . . . Douglas Fir
  - Grade . . . . . No. 1
  - Spacing . . . . . 10 ft
- Anchorage Bolts
  - Type . . . . . ASTM A307, Galvanized
  - Size . . . . . Four ¾-in. ϕ Bolts Per Location
  - Length . . . . . 33 in.
- Bridge Deck Installation . . . . . Longitudinal Glulam Timber Bridge Deck Panels
  - Panel Size . . . . . 10¾ in. x 4 ft x 18 ft - 9 in.
  - Material . . . . . West Coast Douglas Fir
  - Grade . . . . . Combination No. 2
- Vehicle Model . . . . . 1985 Ford F-250
  - Curb Weight . . . . . 4,110 lbs
  - Test Inertial Weight . . . . . 4,435 lbs
  - Gross Static Weight . . . . . 4,435 lbs

- Vehicle Speed
  - Impact . . . . . 31.6 mph
  - Exit . . . . . NA
- Vehicle Angle
  - Impact . . . . . 24.3 degrees
  - Exit . . . . . NA
- Vehicle Snagging . . . . . Minor steel rim and undercarriage gouging on the rail
- Vehicle Stability . . . . . Satisfactory but with moderate vaulting on traffic-side face of bridge railing
- Occupant Ridedown Deceleration (0.010-sec average)
  - Longitudinal . . . . . 7.1 G's ≤ 20 G's
  - Lateral . . . . . 4.1 G's ≤ 20 G's
- Occupant Impact Velocity (normalized)
  - Longitudinal . . . . . 3.9 m/s ≤ 12 m/s
  - Lateral . . . . . 3.2 m/s ≤ 12 m/s
- Vehicle Damage . . . . . Minor
  - TAD[22] 1-RFQ-1
  - SAE[23] 01RDWN2
- Vehicle Stopping Distance . . . . . 50 ft
- Barrier Damage . . . . . Minor scrapes and gouges on the rail as well as deformed steel splice plates

- Maximum Rail Deflections
  - Permanent Set . . . . . 0.1 in.
  - Dynamic . . . . . 2.7 in.

(1 in. = 25.4 mm, 1 lb = 0.454 kg, 1 mph = 1.609 kph)

Figure 21. Summary of Test Results and Sequential Photographs, Test CTBR-1

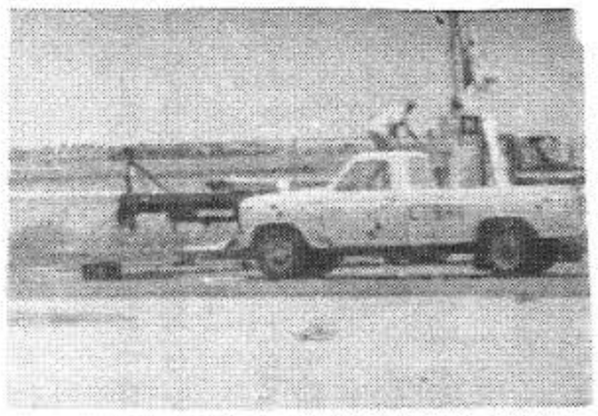

0.000 sec

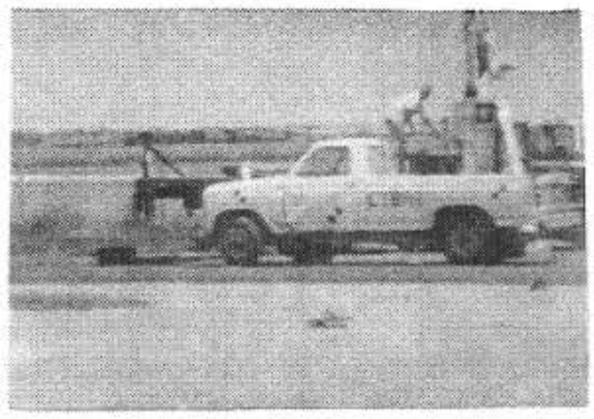

0.059 sec

0.119 sec

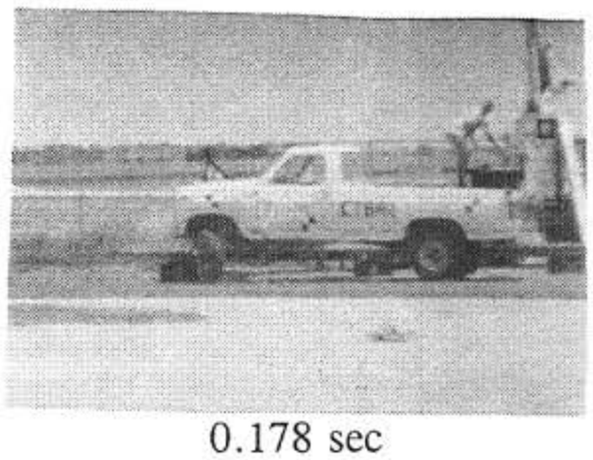

0.178 sec

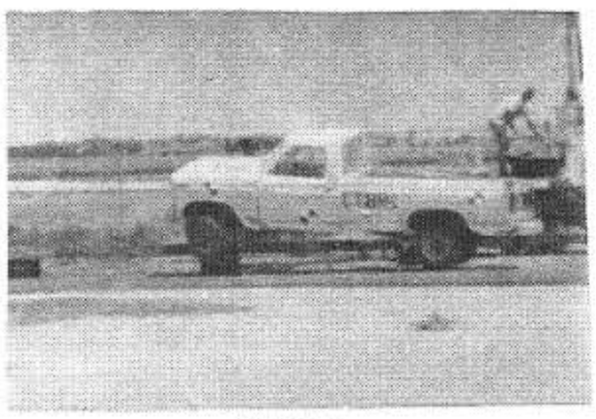

0.237 sec

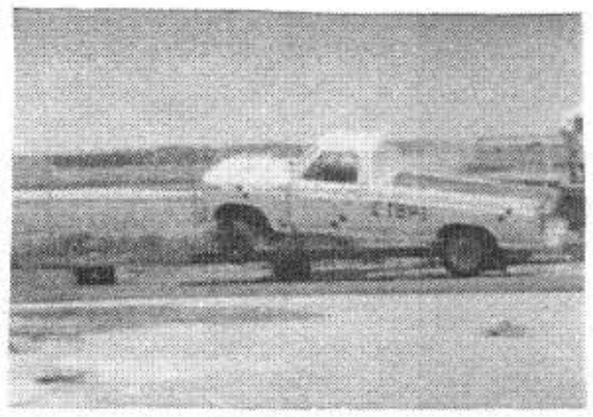

0.296 sec

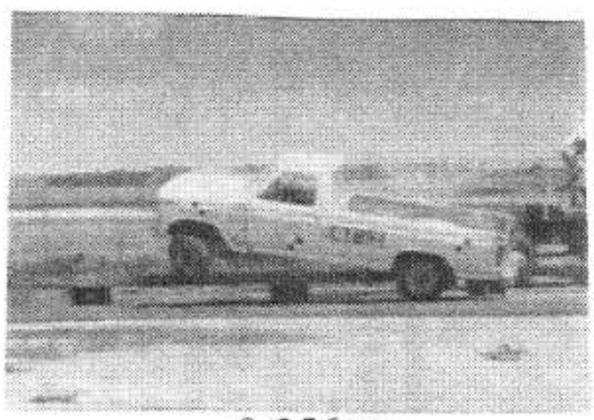

0.356 sec

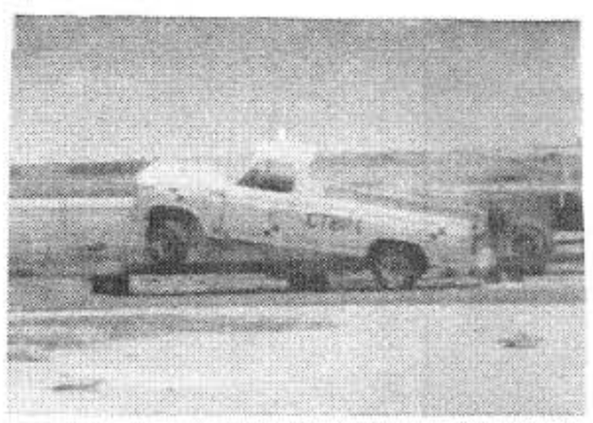

0.415 sec

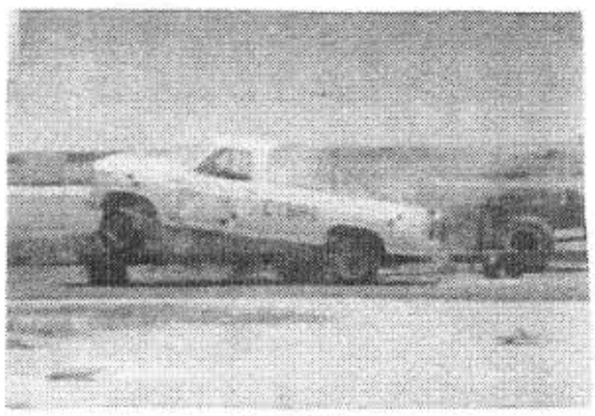

0.474 sec

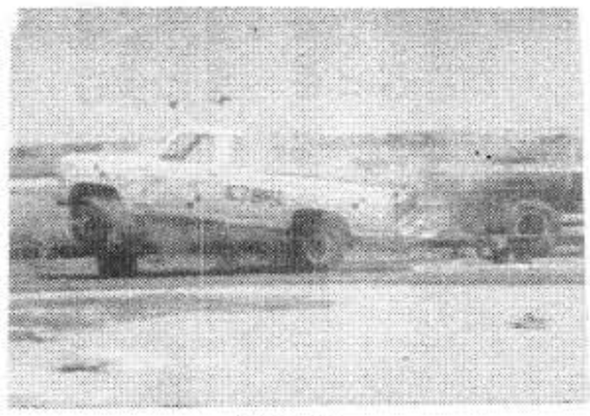

0.533 sec

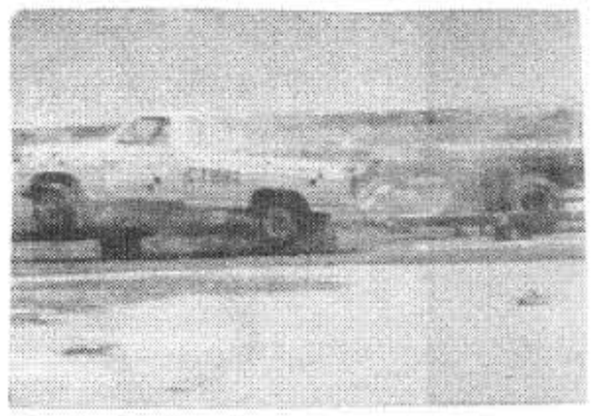

0.593 sec

Figure 22. Additional Sequential Photographs, Test CTBR-1

0.000 sec

0.026 sec

0.171 sec

0.181 sec

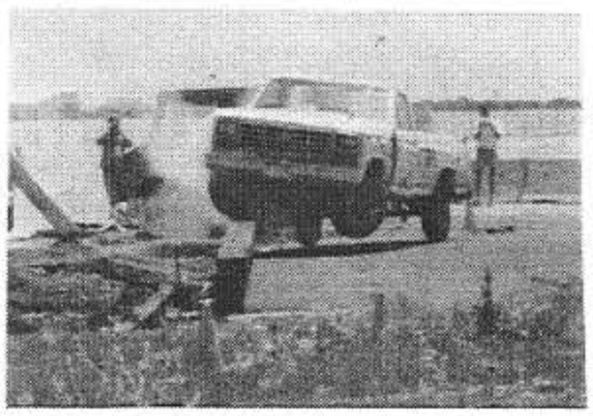

0.231 sec

0.241 sec

0.353 sec

0.422 sec

0.542 sec

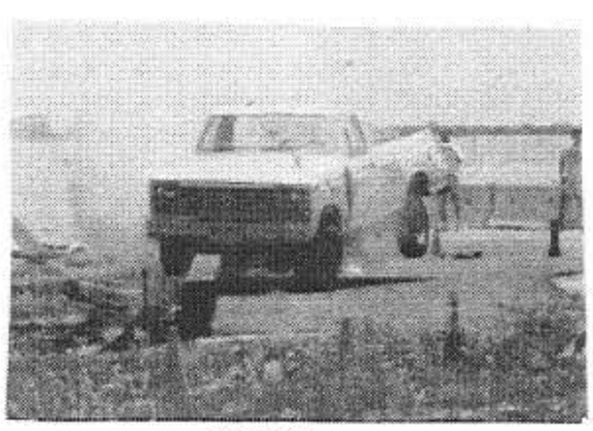

0.723 sec

0.867 sec

Figure 23. Additional Sequential Photographs, Test CTBR-1

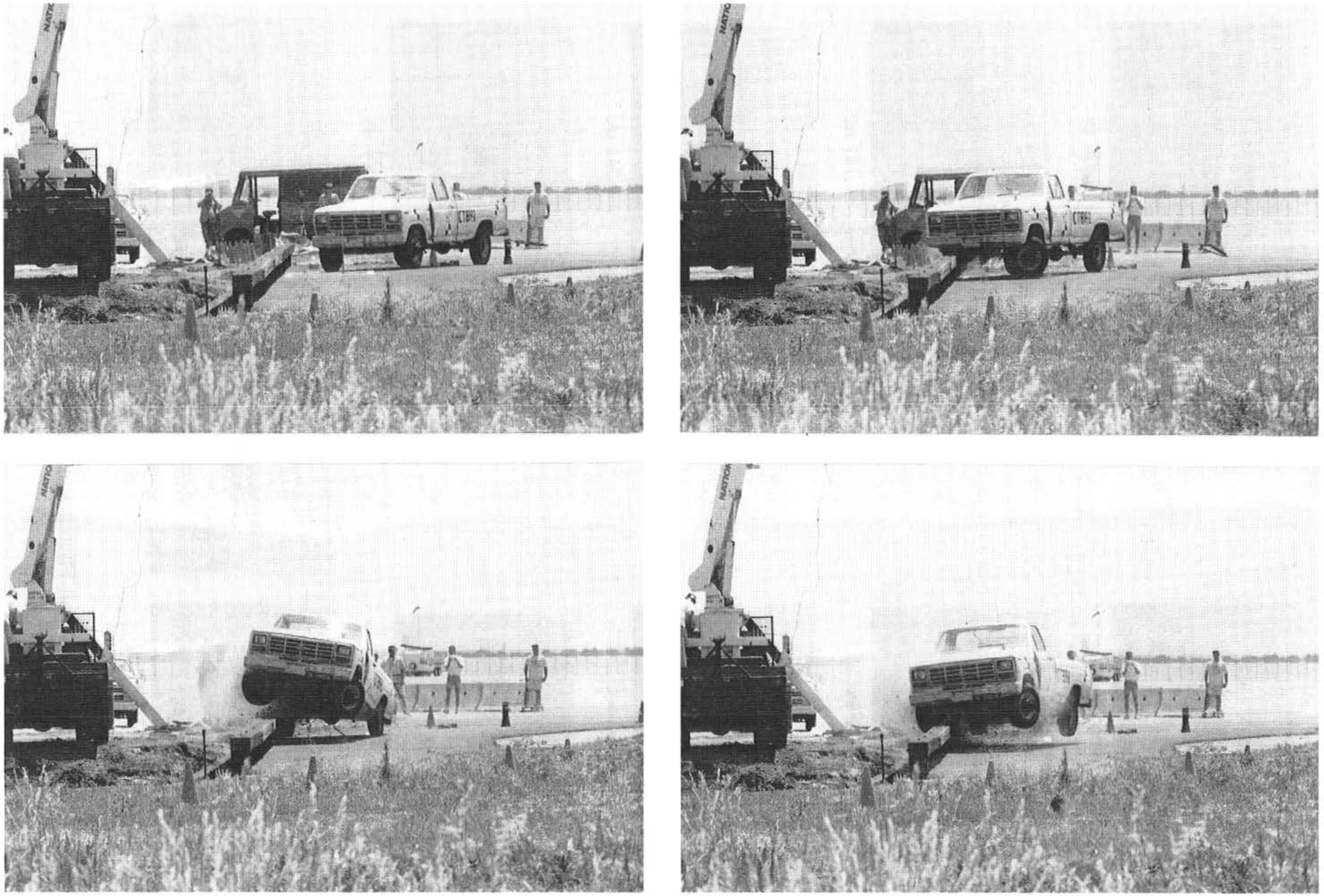

Figure 24. Documentary Photographs, Test CTBR-1

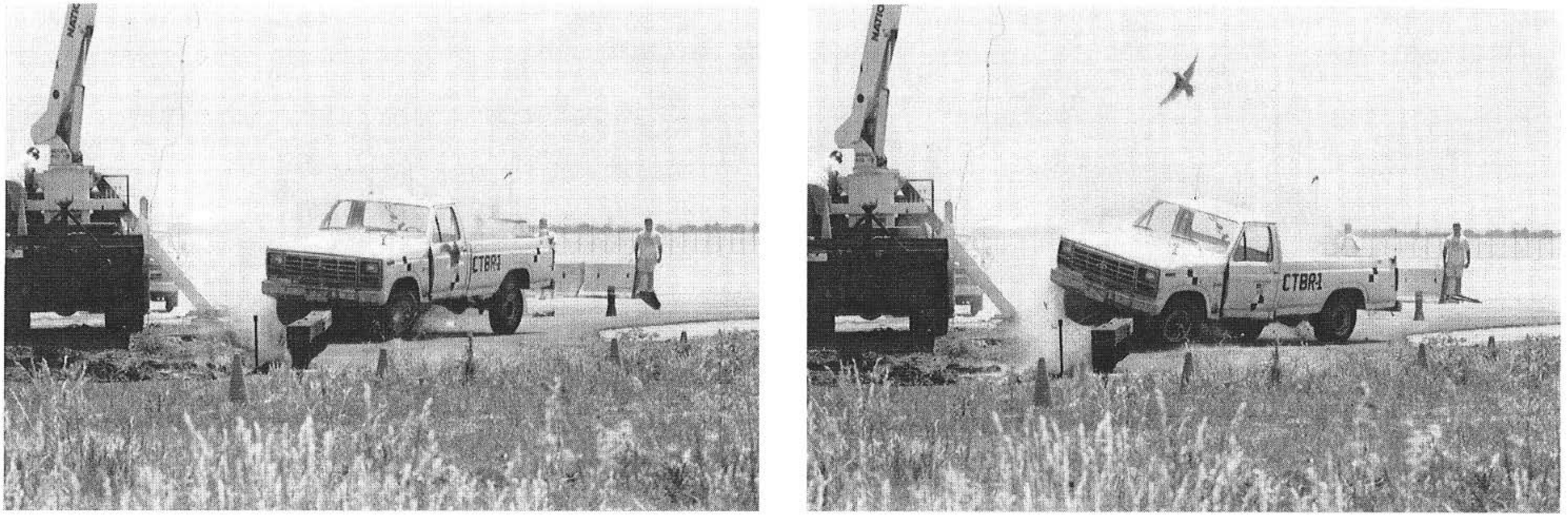

Figure 25. Documentary Photographs, Test CTBR-1

Figure 26. Documentary Photographs, Test CTBR-1

sec and 0.867 sec, the left-front and left-rear tires contacted the deck surface, respectively. At 2.610 sec, the pickup truck came to rest approximately 15.24 m (50 ft) downstream from impact with the front axle on top of the glulam rail and the right-front tire positioned behind the glulam rail, as shown in Figure 27. The vehicle's post-test trajectory is shown in Figure 21.

11.3 Vehicle Damage

Exterior vehicle damage was minor and was limited to deformations of the steel frame and the steel rims of the right-side wheels. The steel frame was shifted slightly due to the oblique impact with the bridge rail. As shown in Figure 28, the right-front and right-rear steel rims were deformed due to the contact with the glulam rail, as evidenced by the wood fibers lodged between the tire and rim and gouges on the face of the glulam rail. Minor undercarriage damage was also observed. No damage occurred to the interior occupant compartment. The vehicle damage was also assessed by the traffic accident scale (TAD) (22) and the vehicle damage index (VDI) (23), as shown in Figure 21.

11.4 Barrier Damage

The minor bridge railing damage is shown in Figures 29 and 30. Scrapes and gouging occurred to the glulam rail along the entire impact distance and on the front, top, and back-side faces of the glulam rail, as shown in Figure 29. As shown in Figure 29, a large scrape and a 19 mm (¾-in.) deep gouge, resulting from the rim-rail contact, was observed on the front face of the glulam rail approximately 203 mm (8 in.) downstream from impact. Damage to the glulam rail was mostly superficial, resulting in little or no compromise of the structural integrity of the bridge rail. The maximum permanent set and dynamic deflections were 3 mm (0.1 in.) and 69 mm (2.7 in.), respectively. The steel splice plate connection located at the midspan

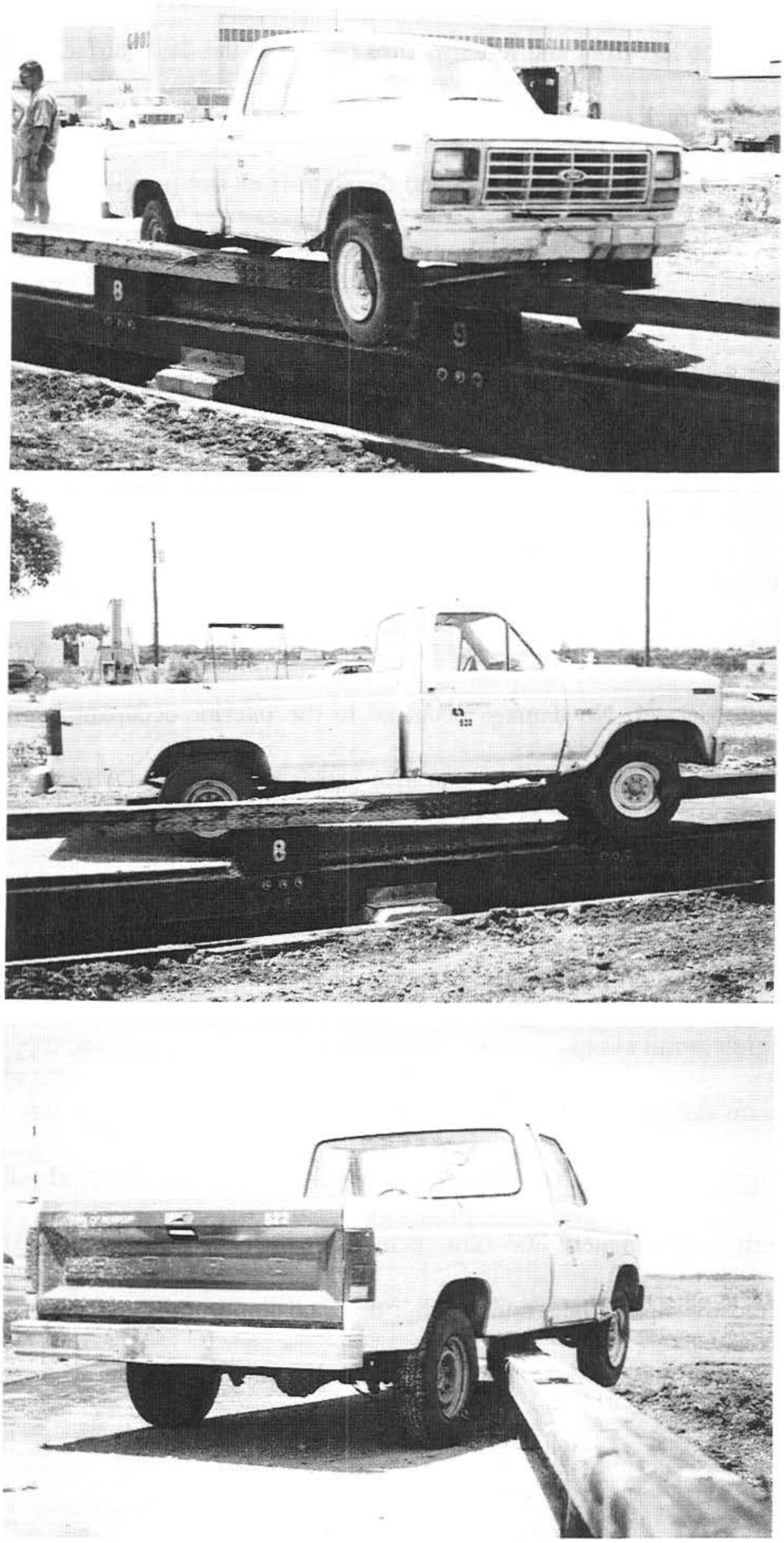

Figure 27. Vehicle Position at Rest, Test CTBR-1

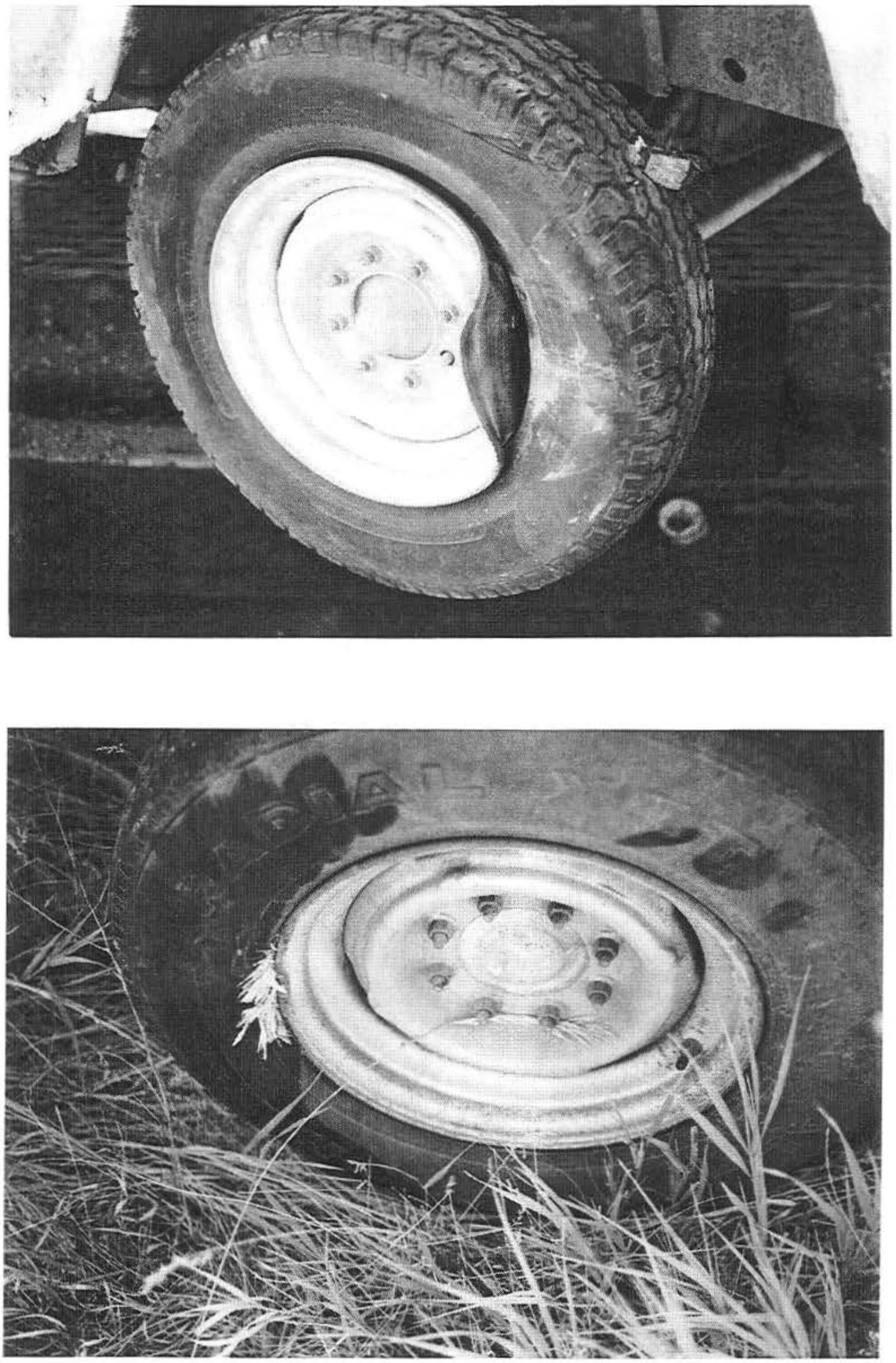

Figure 28. Steel Rim Deformations, Test CTBR-1

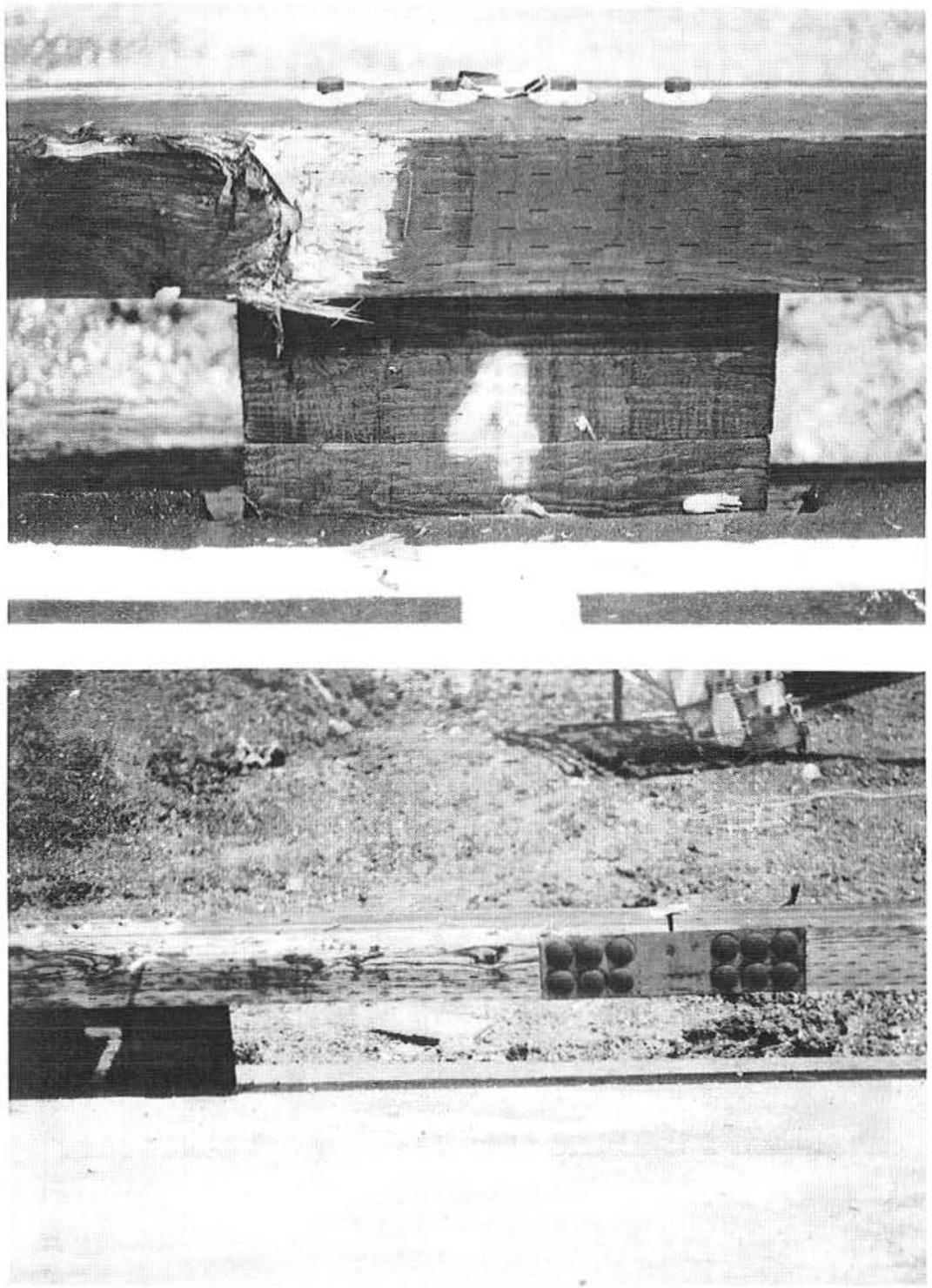

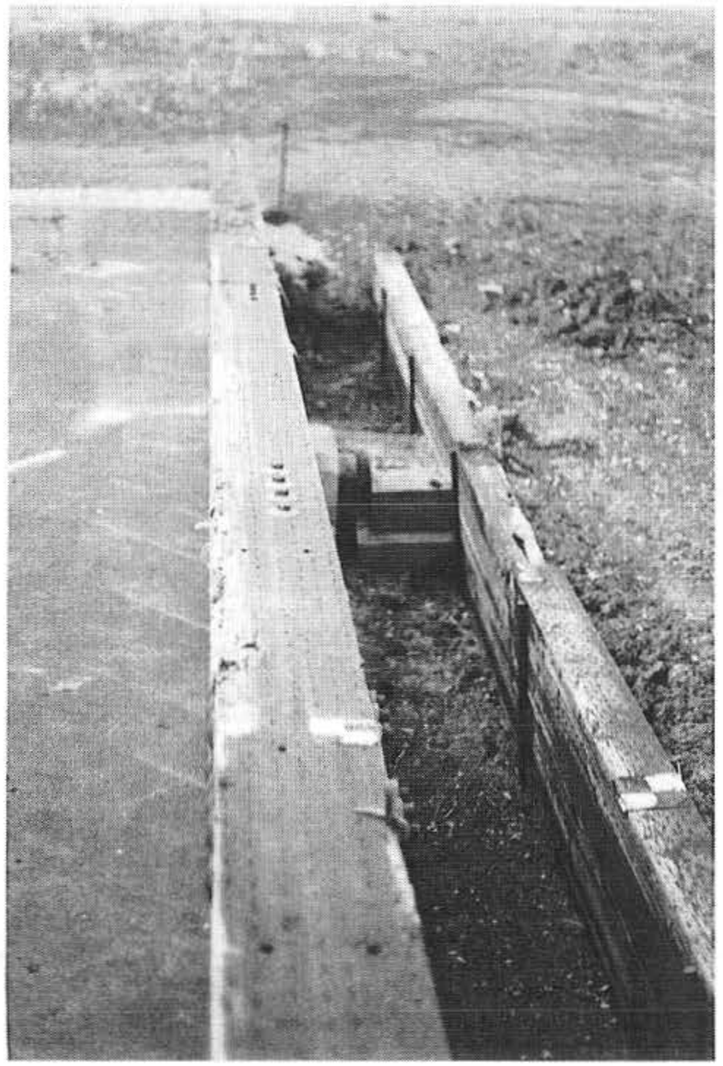

Figure 29. Glulam Rail Damage, Test CTBR-1

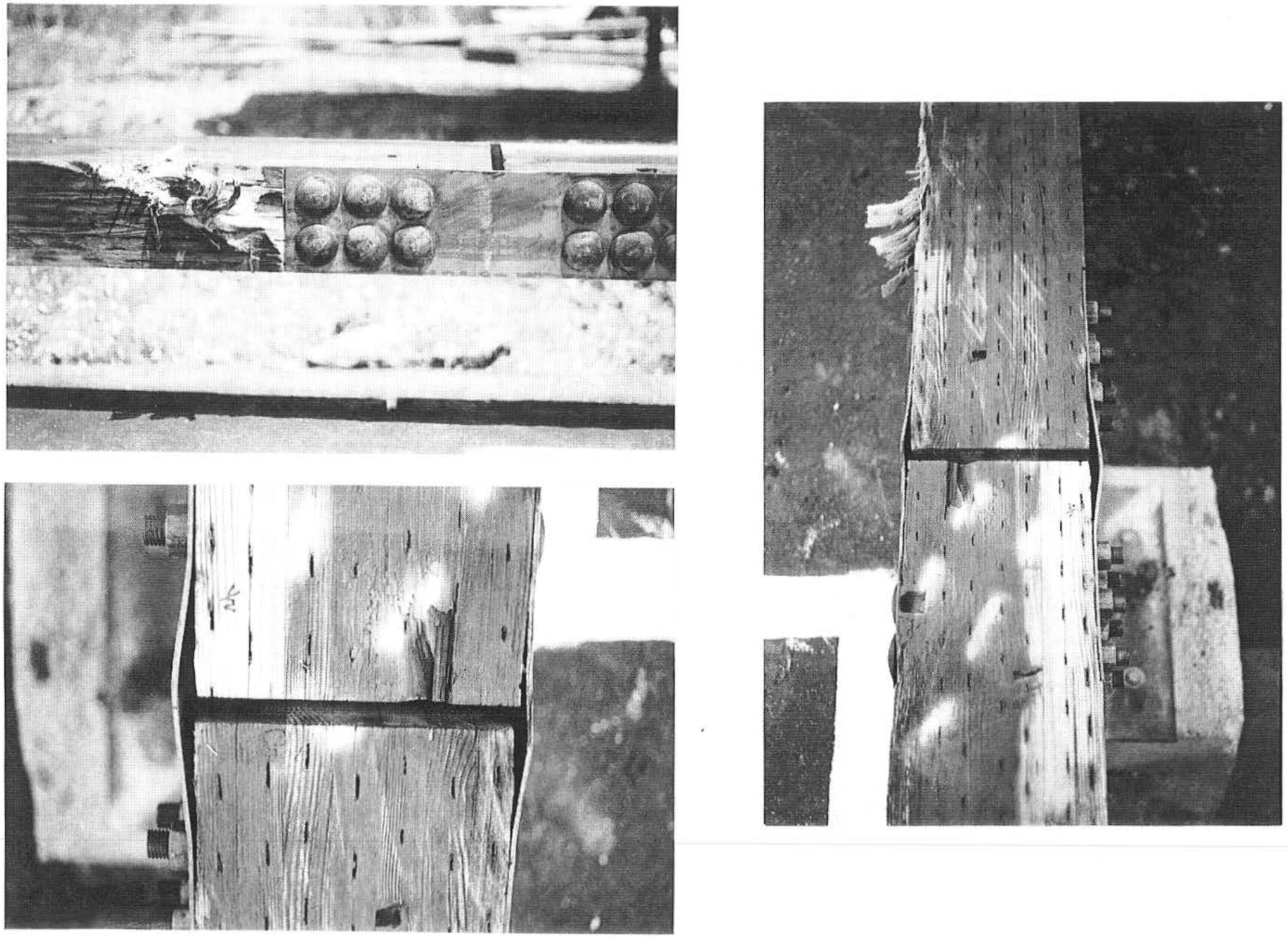

Figure 30. Damage to Glulam Rail and Splice Plate Connection, Test CTBR-1

between post nos. 4 and 5 was deformed, as shown in Figure 30. Figure 30 also shows a gouge which occurred on the face of the glulam rail and downstream of the steel splice plate from the impact of the right-rear steel rim. No damage occurred to the deck, lag screws, or scupper blocks.

11.5 Occupant Risk Values

The normalized longitudinal and lateral occupant impact velocities were determined to be 12.8 ft/sec (3.9 m/sec) and 10.6 ft/sec (3.2 m/sec), respectively. The maximum 0.010-sec average occupant ridedown decelerations in the longitudinal and lateral directions were 7.1 g's and 4.1 g's, respectively. The results of the occupant risk, determined from accelerometer data, are summarized in Figure 21. Results are shown graphically in Appendix C.

12 DISCUSSION AND CONCLUSIONS

A low-cost, low-height curb-type bridge railing, consisting of a glulam timber rail, sawn lumber scupper blocks, and steel splice plates, was developed and full-scale crash tested for use on longitudinal glulam timber decks with low traffic volumes and speeds. One full-scale vehicle crash test, test CTBR-1, was performed and determined to have acceptable safety performance according to TL-1 of NCHRP Report No. 350 (1). A summary of the safety performance evaluation is provided in Table 5.

The development of the timber, curb-type bridge railing addressed the concerns for aesthetics, economy, material availability, and ease of construction. Material costs for the bridge railing can be expected to range between $30 and $40 per lineal foot. In addition, the curb-type bridge railing system was relatively easy to install and should have low construction labor costs. This railing system should also be adaptable to other types of longitudinal decks with little or no modification.

During the pickup truck crash test, the right-front wheel climbed, traversed, and extended over the glulam rail. However, it was determined that the pickup truck did not show any potential for vaulting over the railing system. In addition, the pickup truck was brought to a controlled and stable stop with three wheels positioned on the surface of the bridge deck. Therefore, the successful completion of this research project resulted in a curb-type bridge railing having acceptable safety performance and meeting current crash test safety standards.

Table 5. Summary of Safety Performance Evaluation

Evaluation Factors	Evaluation Criteria	Test CTBR-1
Structural Adequacy	A. Test article should contain and redirect the vehicle; the vehicle should not penetrate, underride, or override the installation although controlled lateral deflection of the test article is acceptable.	S
Occupant Risk	D. Detached elements, fragments or other debris from the test article should not penetrate or show potential for penetrating the occupant compartment, or present an undue hazard to other traffic, pedestrians, or personnel in a work zone. Deformations of, or intrusions into, the occupant compartment that could cause serious injuries should not be permitted.	S
	F. The vehicle should remain upright during and after collision although moderate roll, pitching and yawing are acceptable.	S
Vehicle Trajectory	K. After collision it is preferable that the vehicle's trajectory not intrude into adjacent traffic lanes.	S
	L. The occupant impact velocity in the longitudinal direction should not exceed 12 m/sec and the occupant ridedown acceleration in the longitudinal direction should not exceed 20 G's.	S
	M. The exit angle from the test article preferably should be less than 60 percent of test impact angle, measured at time of vehicle loss of contact with test devise.	S

S - (Satisfactory)
U - (Unsatisfactory)

13 RECOMMENDATIONS

The curb-type bridge railing described herein was developed for use on low service-level roadways with low impact requirements (i.e., TL-1 of NCHRP 350). However, the results of this research study indicate that curb-type railing systems could be developed for use on medium service-level roadways and work-zones with moderate impact requirements, such as TL-2 of NCHRP 350. This increase in performance level may be obtained by (1) increasing the top mounting height of the curb by 4 to 6 in., (2) increasing the size of the glulam rail as well as the overhang distance, and (3) modifying the post to deck attachment. However, these design modifications can only be verified through the use of full-scale vehicle crash testing.

Within the funding limits of this research study, it was not possible to address the concern of an errant vehicle impacting the end of the railing system. Thus, it is recommended that a research study be initiated to develop and evaluate a low-cost end treatment for use with the curb-type bridge railing.

14 REFERENCES

1. Ross, H.E., Sicking, D.L., Zimmer, R.A. and Michie, J.D., *Recommended Procedures for the Safety Performance Evaluation of Highway Features*, National Cooperative Research Program (NCHRP) Report No. 350, Transportation Research Board, Washington, D.C., 1993.

2. *Guide Specifications for Bridge Railings*, American Association of State Highway and Transportation Officials, Washington, D.C., 1989.

3. Faller, R.K., Ritter, M.A., Holloway, J.C., Pfeifer, B.G., and B.T. Rosson, *Performance Level 1 Bridge Railings for Timber Decks*, Transportation Research Record No. 1419, Transportation Research Board, National Research Council, Washington D.C., 1993.

4. Ritter, M.A., Lee, P.D.H., Faller, R.K., Rosson, B.T., and S.R. Duwaldi, *Plans for Crash Tested Bridge Railings for Longitudinal Wood Decks*, General Technical Report No. FPL-GTR-87, United States Department of Agriculture, Forest Service, Forest Products Laboratory, Madison, Wisconsin, September 1995.

5. Ritter, M.A. and R.K. Faller, *Crashworthy Bridge Railings for Longitudinal Wood Decks*, Paper presented by Ritter at the 1994 Pacific Timber Engineering Conference, Gold Coast, Australia, July 11-15, 1994.

6. Ritter, M.A., Faller, R.K., and Duwaldi, S.R., *Crash-Tested Bridge Railings for Timber Bridges*, Presented by Ritter at the Fourth International Bridge Engineering Conference, Volume 2, Conference Proceedings 7, San Francisco, California, August 28-30, 1995, Transportation Research Board, Washington, D.C.

7. Rosson, B.T., Faller, R.K., and M.A. Ritter, *Performance Level 2 and Test Level 4 Bridge Railings for Timber Decks*, Transportation Research Record No. 1500, Transportation Research Board, National Research Council, Washington D.C., 1995.

8. Faller, R.K., Rosson, B.T., Ritter, M.A., and Sicking, D.L., *Design and Evaluation of Two Low-Volume Bridge Railings*, Presented at the Sixth International Conference on Low-Volume Roads, Volume 2, Conference Proceedings 6, University of Minnesota, Minneapolis, Minnesota, June 25-29, 1995, Transportation Research Board, Washington, D.C.

9. Hancock, K.L., Hansen, A.G. and J.B. Mayer, *Aesthetic Bridge Rails, Transitions, and Terminals for Park Roads and Parkways*, Report No. FHWA-RD-90-052, Submitted to the Office of Safety and Traffic Operations R&D, Federal Highway Administration, Performed by the Scientex Corporation, May 1990.

10. Raju, P.R., GangaRao, H.V.S., Mak, K.K. and D.C. Alberson, *Timber Bridge Rail Testing and Evaluation: Timber Bridge Rail, Posts, and Deck on Steel Stringers*, Final Report, Volume 1, Constructed Facilities Center, West Virginia University, Morgantown, WV, October 1993.

11. Raju, P.R., GangaRao, H.V.S., Mak, K.K. and D.C. Alberson, *Timber Bridge Rail and Transition Rail Testing and Evaluation: Glulam Bridge Rail and Deck on Glulam Stringers*, Final Report, Volume 2, Constructed Facilities Center, West Virginia University, Morgantown, WV, October 1993.

12. Raju, P.R., GangaRao, H.V.S., Mak, K.K. and D.C. Alberson, *Timber Bridge Rail and Transition Rail Testing and Evaluation: W-Beam Steel Rail, Timber Posts and Glulam Deck on Steel Stringers*, Final Report, Volume 3, Constructed Facilities Center, West Virginia University, Morgantown, WV, October 1993.

13. Raju, P.R., GangaRao, H.V.S., Duwaldi, S.R. and H.K. Thippeswamy, *Development and Testing of Timber Bridge and Transition Rails for Transverse Glued-Laminated Bridge Decks*, Transportation Research Record No. 1460, Transportation Research Board, National Research Council, Washington D.C., 1994.

14. Bronstad, M.E., and Kimball, C.E., *Crash Test Evaluation of Temporary Traffic Barriers*, Transportation Research Record No. 693, Transportation Research Board, National Research Council, Washington D.C., 1978.

15. Hahn, K.C., and Bryden, J.E., *Crash Tests of Construction-Zone Traffic Barriers*, Transportation Research Record No. 769, Transportation Research Board, National Research Council, Washington D.C., 1980.

16. *Tentative Service Requirements For Bridge Rail Systems*, National Cooperative Highway Research Program (NCHRP) Report 86, Highway Research Board, National Research Council, Washington, D.C., 1970.

17. *Guide for Selecting, Locating, and Designing Traffic Barriers*, American Association of State Highway and Transportation Officials, Washington, D.C., 1977.

18. Powell, G.H., *BARRIER VII: A Computer Program For Evaluation of Automobile Barrier Systems*, Prepared for: Federal Highway Administration, Report No. FHWA RD-73-51, April 1973.

19. *American Wood-Preservers' Association Book of Standards*, American Wood-Preservers' Association, Woodstock, Md., 1991.

20. Hinch, J., Yang, T-L, and Owings, R., *Guidance Systems for Vehicle Testing*, ENSCO, Inc., Springfield, VA, 1986.

21. Taborck, J.J., "*Mechanics of Vehicles - 7*", Machine Design Journal, May 30, 1957.

22. *Vehicle Damage Scale for Traffic Investigators*, Second Edition, Technical Bulletin No. 1, Traffic Accident Data (TAD) Project, National Safety Council, Chicago, Illinois, 1971.

23. *Collision Deformation Classification - Recommended Practice J224 March 1980*, Handbook Volume 4, Society of Automotive Engineers (SAE), Warrendale, Pennsylvania, 1985.

15 APPENDICES

APPENDIX A - BARRIER VII COMPUTER MODEL

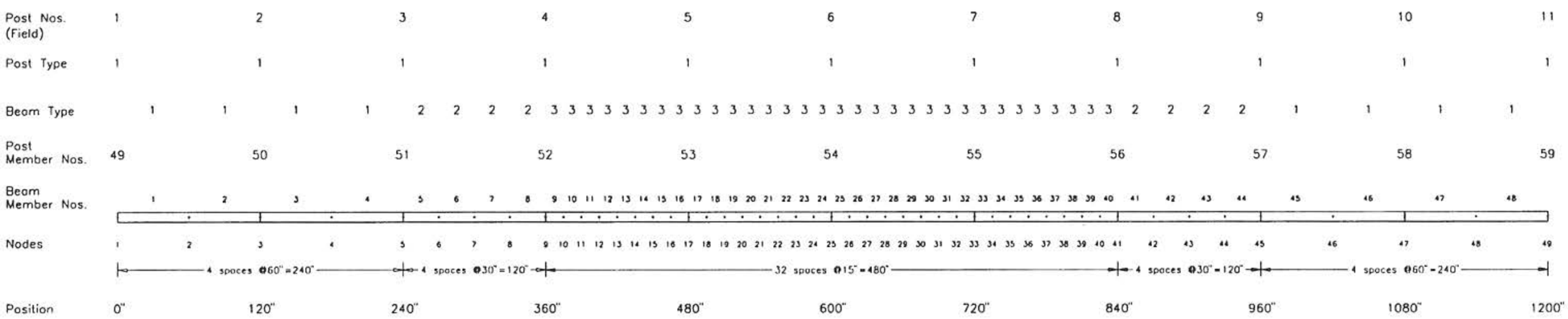

Figure A-1. Finite Element Model of the Curb-Type Bridge Railing

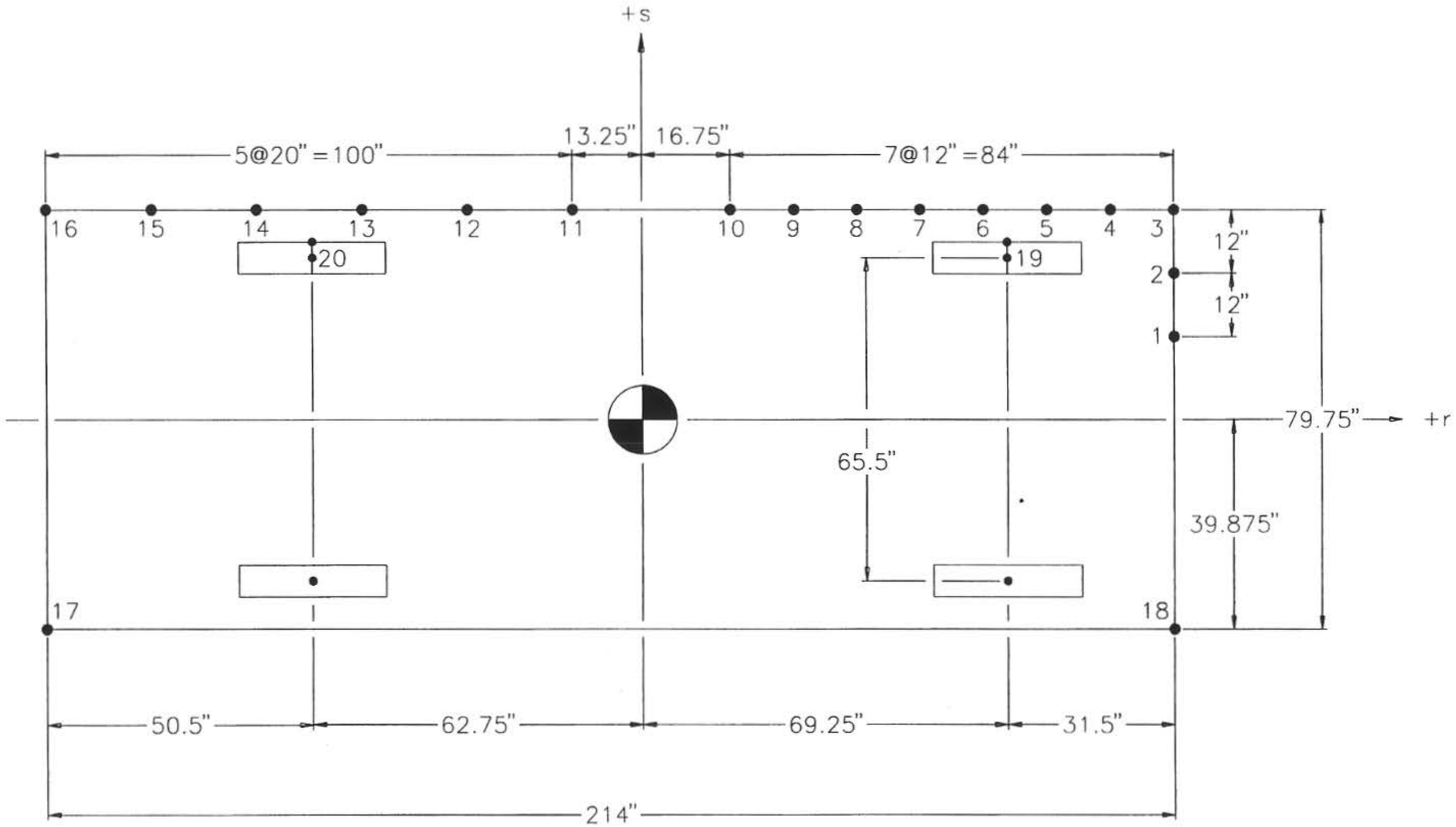

Figure A-2. Idealized finite element, 2 dimensional vehicle model for the 2,000-kg pickup truck

APPENDIX B - BARRIER VII INPUT FILE

```
TL-1 CURB-TYPE BRIDGE RAILING WITH 4400-LB PICKUP TRUCK, 31.07 MPH, 25 DEG, NODE 19
   49    6    5    1   59    8    2    0
    0.0010    0.0010      0.80  100    0       1.0    1
    1    5    5    5    5    5    1
    1       0.0       0.0
    5     240.0       0.0
    9     360.0       0.0
   41     840.0       0.0
   45     960.0       0.0
   49    1200.0       0.0
    1    5    3    1       0.0
    5    9    3    1       0.0
    9   41   31    1       0.0
   41   45    3    1       0.0
   45   49    3    1       0.0
    1   49      0.45
   49   48   47   46   45   44   43   42   41   40
   39   38   37   36   35   34   33   32   31   30
   29   28   27   26   25   24   23   22   21   20
   19   18   17   16   15   14   13   12   11   10
    9    8    7    6    5    4    3    2    1
  100    3
    1    651.16    70.875     60.00    1680.0      24.6    206.99     653.0 0.10
    2    651.16    70.875     30.00    1680.0      24.6    206.99     653.0 0.10
    3    651.16    70.875     15.00    1680.0      24.6    206.99     653.0 0.10
  300    1
    1    16.375       0.0     10.00      4.53      87.9    409.38    178.13 0.10
      30.0      15.0      1.0      6.5
    1    1    2    4    1  101       0.0       0.0       0.0
    5    5    6    8    1  102       0.0       0.0       0.0
    9    9   10   40    1  103       0.0       0.0       0.0
   41   41   42   44    1  102       0.0       0.0       0.0
   45   45   46   48    1  101       0.0       0.0       0.0
   49    1       51    2  301       0.0       0.0       0.0       0.0       0.0
   52    9       56    8  301       0.0       0.0       0.0       0.0       0.0
   57   45       59    2  301       0.0       0.0       0.0       0.0       0.0
   4400.0   40000.0   20    6    4    0    1
    1     0.055      0.12      6.00      17.0
    2     0.057      0.15      7.00      18.0
    3     0.062      0.18     10.00      12.0
    4     0.110      0.35     12.00       6.0
    5      0.35      0.45      6.00       5.0
    6      1.45      1.50     15.00       1.0
    1    100.75    15.875    1      12.0    1    0    0    0
    2    100.75    27.875    1      12.0    0    0    0    0
    3    100.75    39.875    2      12.0    0    0    0    0
    4     88.75    39.875    2      12.0    0    0    0    0
    5     76.75    39.875    2      12.0    0    0    0    0
    6     64.75    39.875    2      12.0    0    0    0    0
    7     52.75    39.875    2      12.0    0    0    0    0
    8     40.75    39.875    2      12.0    0    0    0    0
    9     28.75    39.875    2      12.0    0    0    0    0
   10     16.75    39.875    2      12.0    0    0    0    0
   11    -13.25    39.875    3      12.0    0    0    0    0
   12    -33.25    39.875    3      12.0    0    0    0    0
   13    -53.25    39.875    3      12.0    0    0    0    0
   14    -73.25    39.875    3      12.0    0    0    0    0
   15    -93.25    39.875    3      12.0    0    0    0    0
   16   -113.25    39.875    4      12.0    0    0    0    0
   17   -113.25   -39.875    4      12.0    0    0    0    0
```

```
18     100.75    -39.875    1        12.0     0     0     0     0
19      69.25     37.75     5         1.0     1     0     0     0
20     -62.75     37.75     6         1.0     1     0     0     0
 1      69.25     37.75          0.0          608.
 2      69.25    -37.75          0.0          608.
 3     -62.75     37.75          0.0          492.
 4     -62.75    -37.75          0.0          492.
 1        0.0       0.0
19      510.0       0.0       25.0          31.07          0.0          0.0          1.0
```

APPENDIX C - ACCELEROMETER DATA ANALYSIS

ACCELEROMETER DATA ANALYSIS, CTBR-1

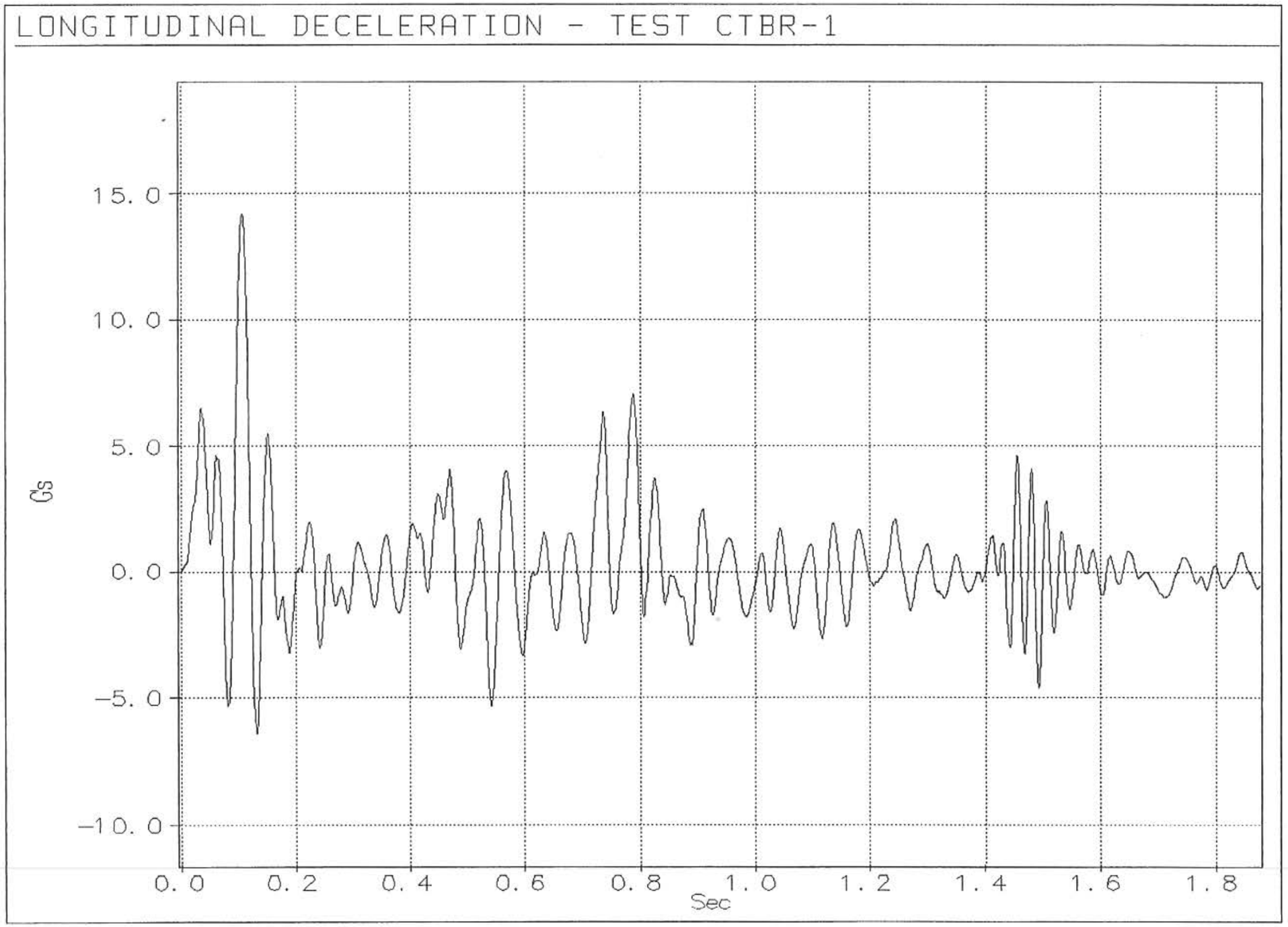

Figure C-1. Graph of Longitudinal Deceleration, Test CTBR-1

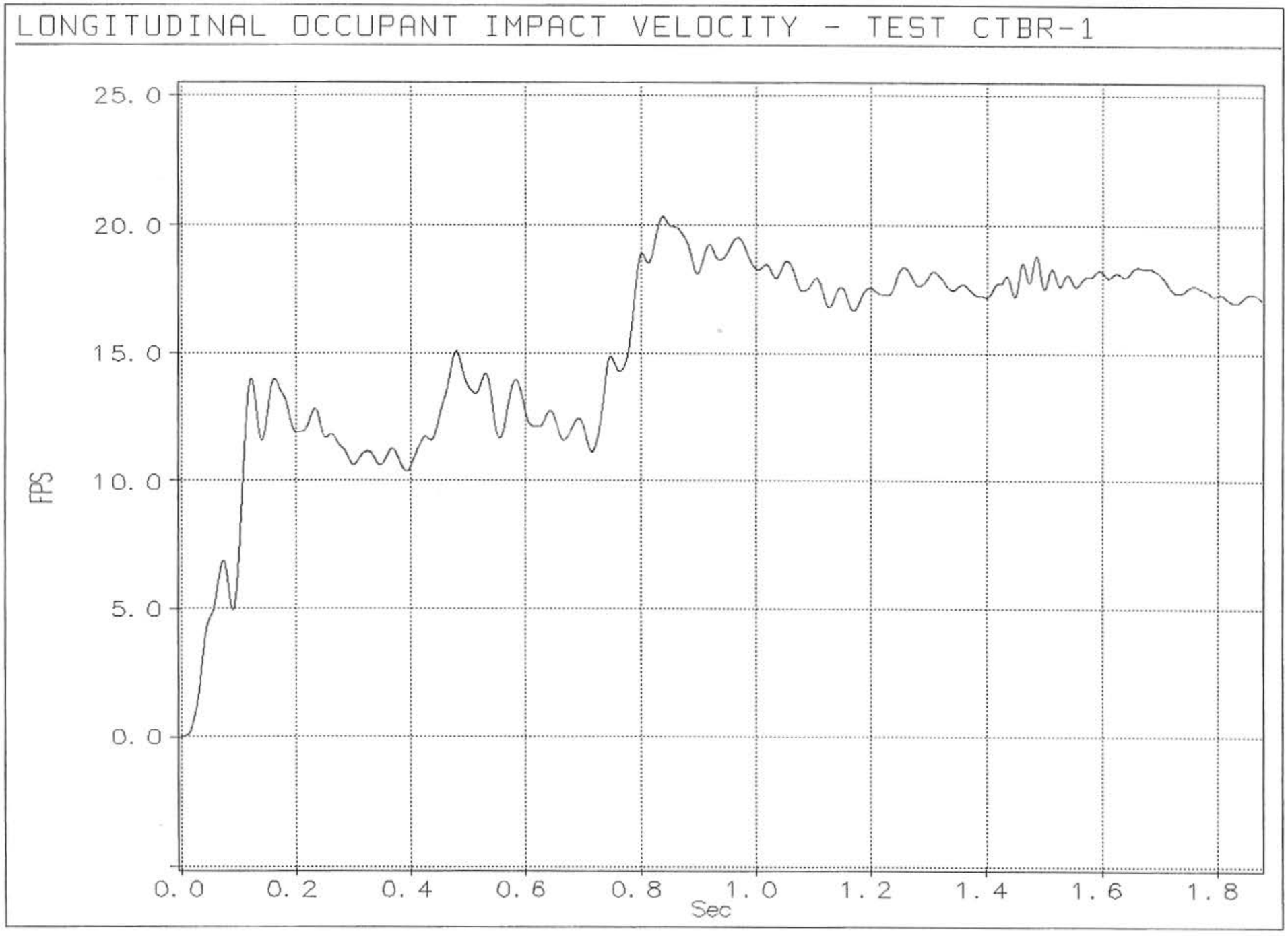

Figure C-2. Graph of Longitudinal Occupant Impact Velocity, Test CTBR-1

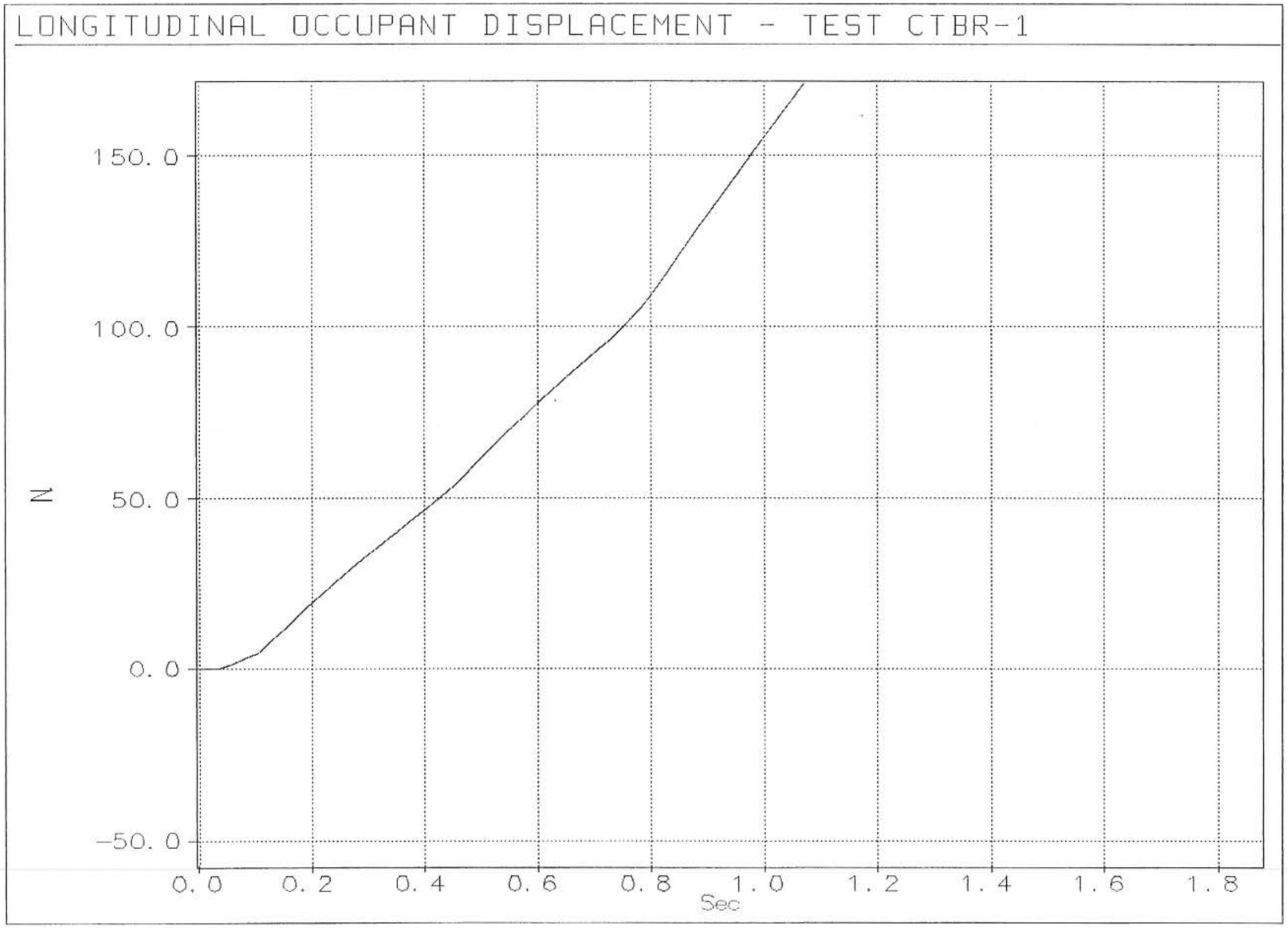

Figure C-3. Graph of Longitudinal Occupant Displacement, Test CTBR-1

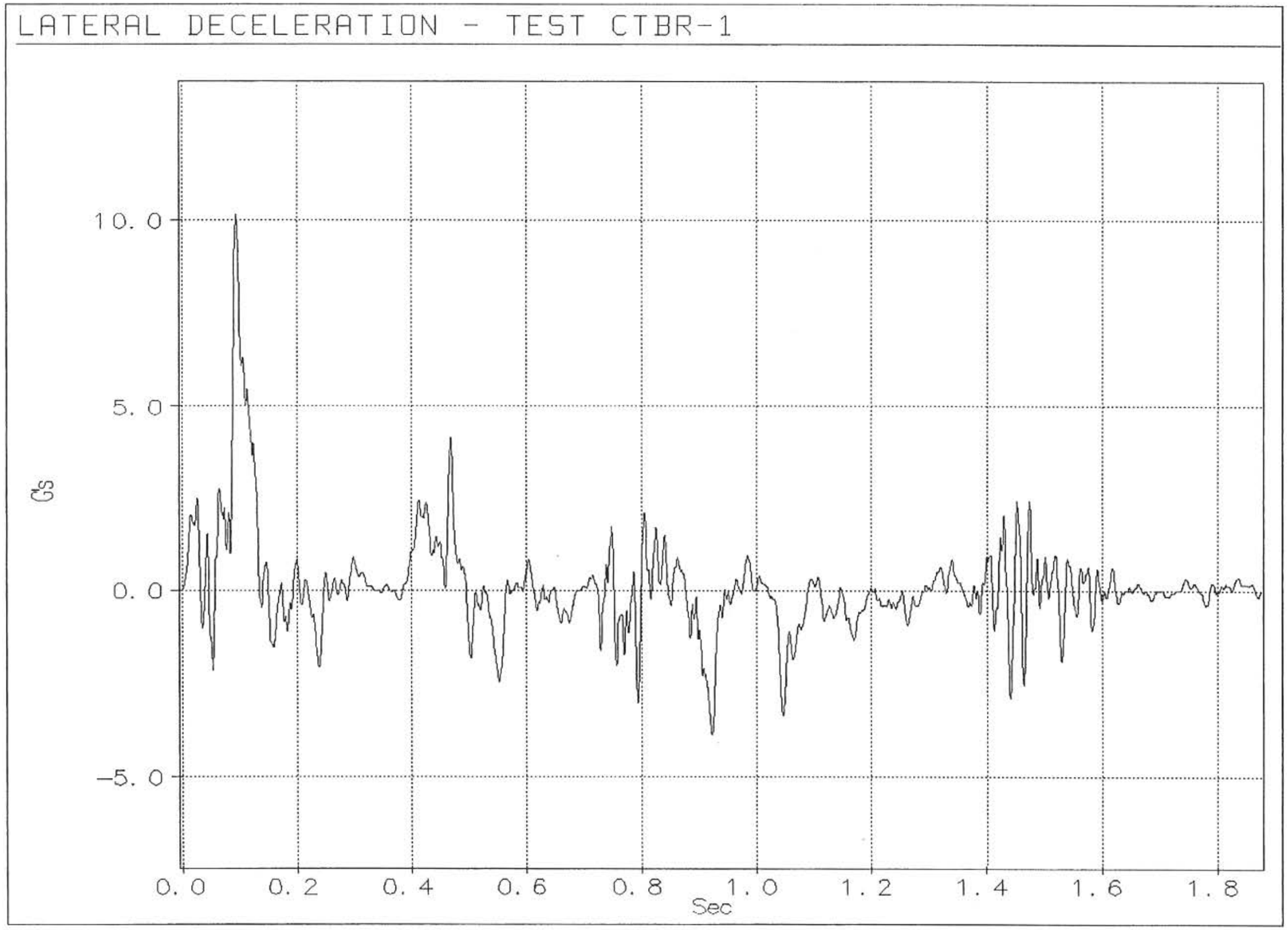

Figure C-4. Graph of Lateral Deceleration, Test CTBR-1

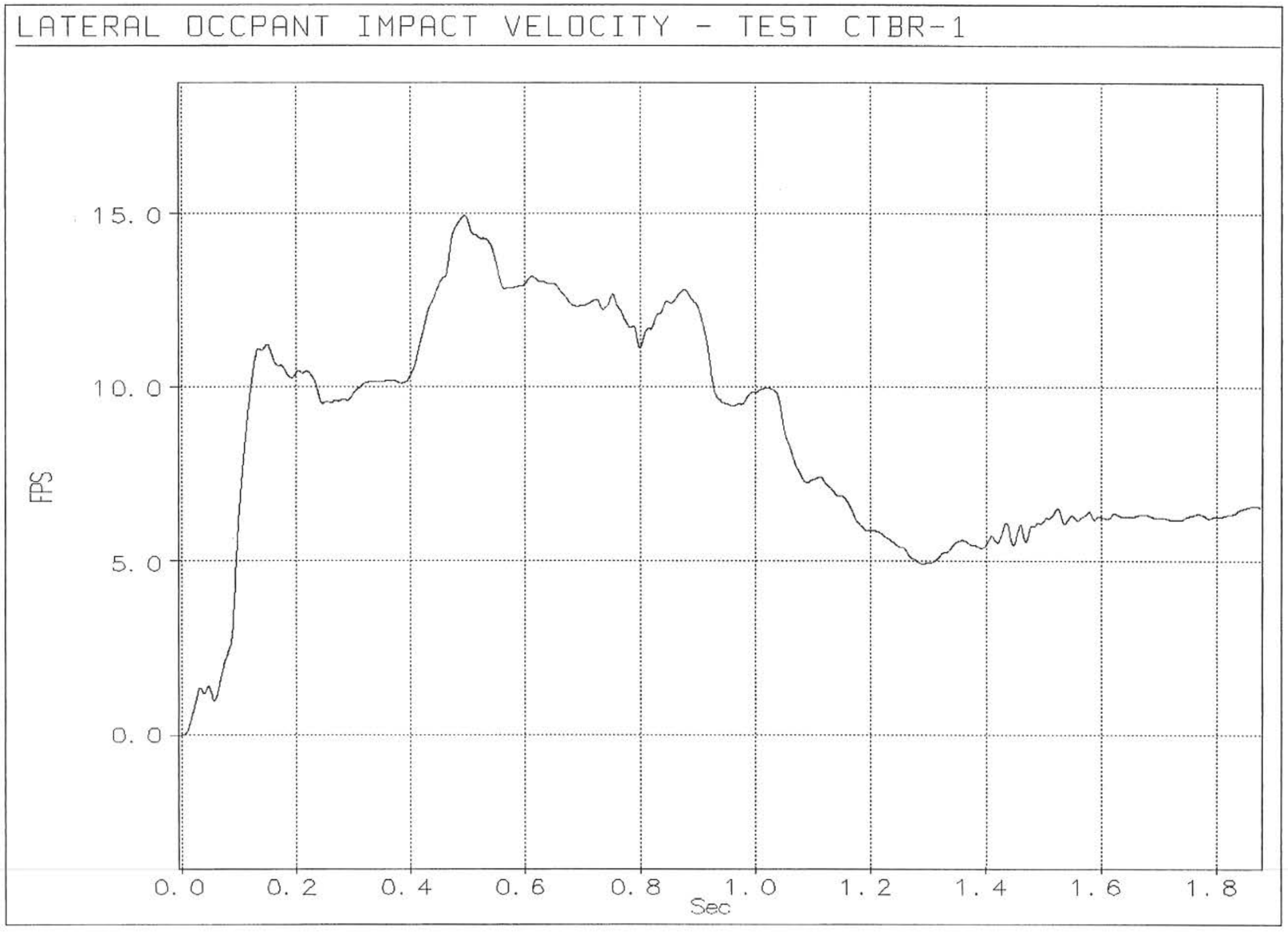

Figure C-5. Graph of Lateral Occupant Impact Velocity, Test CTBR-1

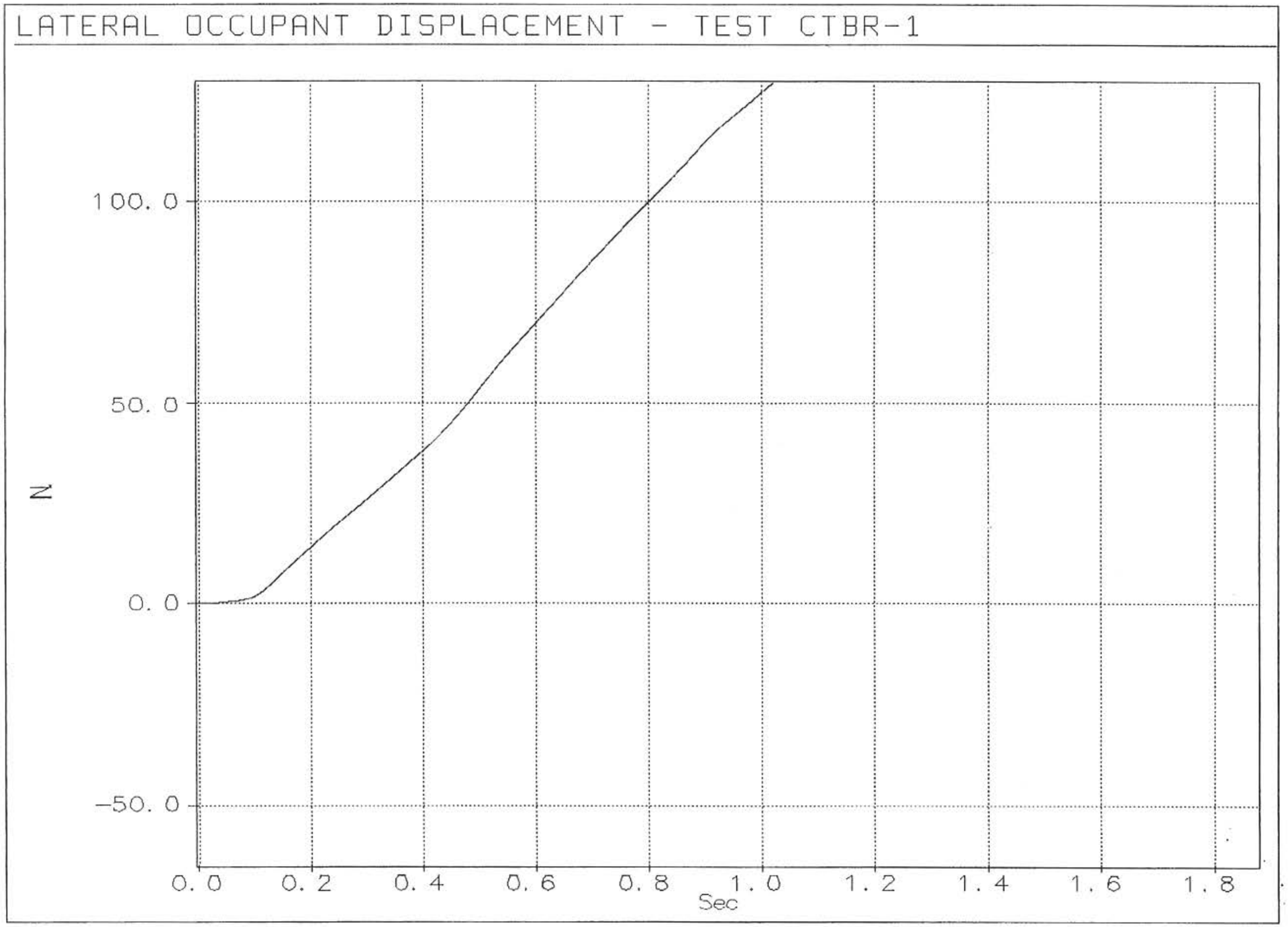

Figure C-6. Graph of Lateral Occupant Displacement, Test CTBR-1